

cy. 2



**DESIGN ASSURANCE TEST OF THE THIOKOL TE-M-521-5  
APOGEE KICK MOTOR TESTED IN THE SPIN MODE  
AT SIMULATED ALTITUDE CONDITIONS**

**A. A. Cimino**

**ARO, Inc.**

**March 1973**

Approved for public release; distribution unlimited.

**ENGINE TEST FACILITY  
ARNOLD ENGINEERING DEVELOPMENT CENTER  
AIR FORCE SYSTEMS COMMAND  
ARNOLD AIR FORCE STATION, TENNESSEE**

# ***NOTICES***

When U. S. Government drawings, specifications, or other data are used for any purpose other than a definitely related Government procurement operation, the Government thereby incurs no responsibility nor any obligation whatsoever, and the fact that the Government may have formulated, furnished, or in any way supplied the said drawings, specifications, or other data, is not to be regarded by implication or otherwise, or in any manner licensing the holder or any other person or corporation, or conveying any rights or permission to manufacture, use, or sell any patented invention that may in any way be related thereto.

Qualified users may obtain copies of this report from the Defense Documentation Center.

References to named commercial products in this report are not to be considered in any sense as an endorsement of the product by the United States Air Force or the Government.

**DESIGN ASSURANCE TEST OF THE THIOKOL TE-M-521-5  
APOGEE KICK MOTOR TESTED IN THE SPIN MODE  
AT SIMULATED ALTITUDE CONDITIONS**

**A. A. Cimino  
ARO, Inc.**

Approved for public release; distribution unlimited.

## FOREWORD

The test program reported herein was conducted at the Arnold Engineering Development Center under the sponsorship of the National Aeronautics and Space Administration (NASA), Goddard Space Flight Center (GSFC), for the Thiokol Chemical Corporation (TCC), Elkton Division, under Program Element 921E3. . . . .

The results of the test were obtained by ARO, Inc. (a subsidiary of Sverdrup & Parcel and Associates, Inc.), contract operator of the AEDC, Air Force Systems Command (AFSC), Arnold Air Force Station, Tennessee. The test was conducted in Propulsion Development Test Cell (T-3) of the Engine Test Facility (ETF) on July 28, 1972; under ARO Project No. RA182, and the manuscript was submitted for publication on October 31, 1972.

This technical report has been reviewed and is approved.

CHAUNCEY D. SMITH, JR.  
Lt Colonel, USAF  
Chief Air Force Test Director, ETF  
Directorate of Test

A. L. COAPMAN  
Colonel, USAF  
Director of Test

## ABSTRACT

One Thiokol Chemical Corporation TE-M-521-5 solid-propellant apogee rocket motor was successfully fired at an average simulated altitude of about 108,000 ft while spinning at 46 rpm. The general program objectives were to verify compliance of motor performance with the manufacturer's specifications. Specific primary objectives were to determine vacuum ballistic performance of the motor after prefire vibration conditioning and temperature conditioning at 40°F, altitude ignition characteristics, motor structural integrity, and motor temperature-time history during and after motor operation. Additional objectives were to measure the lateral (nonaxial) thrust component during motor operation and to measure radiation heat flux in the vicinity of the nozzle exit plane.

## CONTENTS

	<u>Page</u>
ABSTRACT . . . . .	iii
NOMENCLATURE . . . . .	vi
I. INTRODUCTION . . . . .	1
II. APPARATUS . . . . .	2
III. PROCEDURE . . . . .	5
IV. RESULTS AND DISCUSSION . . . . .	6
V. SUMMARY OF RESULTS . . . . .	9
REFERENCES . . . . .	10

## APPENDIXES

### I. ILLUSTRATIONS

#### Figure

1. Thiokol Chemical Corporation TE-M-521-5 Solid-Propellant Rocket Motor	
a. Schematic . . . . .	13
b. Photograph (Less Igniters) . . . . .	14
2. Installation of the Thiokol TE-M-521-5 Rocket Motor in Propulsion Développement Test Cell (T-3)	
a. Schematic . . . . .	15
b. Photograph . . . . .	16
c. Details of Nonaxial Force Measuring System . . . . .	17
3. Schematic of Motor Showing Thermocouple Locations . . . . .	18
4. Schematic of Motor Installation Showing Radiometer and Calorimeter Locations . . . . .	19
5. Analog Trace of Motor Ignition Event . . . . .	20
6. Definition of Vacuum Total and Action Impulse . . . . .	21
7. Variation of Thrust, Chamber Pressure, and Test Cell Pressure during Firing . . . . .	22
8. Postfire Photographs of Motor Assembly	
a. Motor Case and Nozzle . . . . .	23
b. Nozzle . . . . .	24
9. Motor Temperature Variation with Time	
a. Motor Case; TC-1, TC-2, and TC-15 . . . . .	25
b. Motor Case; TC-3, TC-4, TC-16, and TC-17 . . . . .	25
c. Motor Case; TC-5, TC-6, TC-18, and TC-19 . . . . .	26
d. Motor Case; TC-7, TC-8, TC-20, and TC-21 . . . . .	26
e. Motor Case; TC-9, TC-10, TC-14, TC-22, and TC-23 . . . . .	27
f. Nozzle; TN-11, TN-12, TN-13, and TN-24 . . . . .	27
10. Exhaust Plume Radiation Variations with Time	
a. Calorimeter, C-1 (View Angle = 140 deg) . . . . .	28
b. Radiometer, R-1 (View Angle = 30 deg) . . . . .	28

<u>Figure</u>	<u>Page</u>
10. (Continued)	
c. Radiometer, R-2 (View Angle = 60 deg) . . . . .	28
d. Radiometer, R-4 (View Angle = 90 deg) . . . . .	29
e. Radiometer, R-5 (View Angle = 3 deg) . . . . .	29
f. Radiometer, R-6 (View Angle = 3 deg) . . . . .	29
11. Space-Time Variation of Magnitude and Angular Position of Lateral (Nonaxial) Thrust Vector	
a. Axial Thrust . . . . .	30
b. Lateral (Nonaxial) Thrust Vector Magnitude . . . . .	30
c. Lateral (Nonaxial) Thrust Vector Angular Position . . . . .	30

## II. TABLES

I. Instrumentation Summary and Measurement Uncertainty . . . . .	31
II. Summary of TE-M-521 Motor Performance . . . . .	32
III. Summary of TE-M-521 Motor Physical Dimensions . . . . .	33

## NOMENCLATURE

$A_{ex}$	Nozzle exit area, in. <sup>2</sup>
$A_t$	Nozzle throat area, in. <sup>2</sup>
$\bar{c}_f$	Average vacuum thrust coefficient over a selected 1-sec interval of motor operation just prior to tailoff
F	Measured axial thrust, lbf
$I_{vac\ action}$	Vacuum impulse based on action time ( $t_a$ ), lbf-sec
$I_{vac\ total}$	Vacuum impulse based on total burn time ( $t_{is}$ ), lbf-sec
$P_{cell}$	Measured cell pressure, psia
$P_{ch}$	Measured chamber pressure, psia
$t_a$	Action time, time interval from 10 percent of maximum chamber pressure at ignition to 10 percent of maximum chamber pressure at tailoff, sec
$t_{bd}$	Time of nozzle flow breakdown, sec
$t_{is}$	Total burn time, time interval between the application of ignition voltage and the time at which the ratio of $P_{ch}$ to $P_{cell}$ has decreased to 1.3 during tailoff, sec

- $t_{\text{g}}$  Ignition lag time, time interval from application of ignition voltage to the first perceptible rise in chamber pressure, sec
- $t_0$  Zero time, time of application of voltage to the igniter, sec

## SECTION I INTRODUCTION

The Thiokol Chemical Corporation (TCC) TE-M-521-5 solid-propellant rocket motor is to be used as the apogee kick motor for the Interplanetary Monitoring Platform (IMP)-H and IMP-J spacecraft (Ref. 1). The kick motor will impart sufficient velocity to inject the spacecraft into a circular orbit at the apogee of its ascent transfer ellipse. The apogee motor is contained within the spacecraft, which is internally insulated with a material designed to protect the communications package from the high temperatures attributable to apogee motor heat soakback (Ref. 1).

The test reported herein was a continuation of the design assurance test program for the TE-M-521-5 motor. An earlier test was conducted at the AEDC on a TE-M-521-5 motor, that had undergone nondestructive vibrational tests at the manufacturer's facilities, which duplicated launch vehicle accelerations (Ref. 2). A subsequent change in the launch vehicle configuration established new requirements for nondestructive vibration tests; these new tests were performed on the motor prior to the motor firing at simulated altitude, reported herein.

The TE-M-521-5 motor is ballistically identical to the earlier models of the TE-M-521 apogee kick motor, used for the Interim Defense Communication Satellite Program (IDCSP/A) spacecraft (Refs. 3 and 4); however, the TE-M-521-5 has a greater minimum wall thickness specification (0.038 in. instead of 0.032 in.) in the forward and aft hemispheres, the nozzle exit cone is fabricated with an additional 0.050-in. phenolic glass cloth overwrap extending 5 in. downstream from the throat, and the Gengard V-44 rubber asbestos propellant-to-case insulation has been replaced with TIR-300 asbestos-polyisoprene.

The general objective of the program reported herein was to verify compliance of motor performance to the manufacturer's specification (Ref. 5). Specific objectives were to determine: (1) the altitude ballistic performance of the TE-M-521-5 rocket motor while spinning about its axial centerline at 46 rpm, after prefire vibration conditioning and temperature conditioning at  $40 \pm 5^\circ\text{F}$  for a minimum of 24 hr, (2) altitude ignition characteristics, (3) motor structural integrity, and (4) motor temperature-time history during and after motor operation. Additional objectives were to measure the lateral (nonaxial) thrust component during motor operation and to measure radiation heat flux in the vicinity of the nozzle exit plane.

Motor altitude ballistic performance, ignition characteristics, structural integrity, motor temperature, exhaust plume heat flux, and motor lateral (nonaxial) thrust are presented and discussed.

## SECTION II APPARATUS

### 2.1 TEST ARTICLE

The Thiokol Chemical Corporation (TCC) TE-M-521-5 solid-propellant rocket motor (Fig. 1, Appendix I) is a full-scale, flightweight motor having the following nominal dimensions and burning characteristics at 40°F:

Length, in.	38.64
Diameter, in.	17.44
Loaded Weight, lbm	275
Propellant Weight, lbm	247
Maximum Thrust, lbf	4000
Maximum Chamber Pressure, psia	706
Action Time, sec	20.0
Throat Area, in.	2.788
Nozzle Area Ratio, $A_{ex}/A_t$	49.11

The elongated spherical motor case is constructed of 0.071-in. forged titanium (6Al-4V) welded to two hemispherical sections of 0.38 in. thickness. The case is lined internally with TCC TL-H-304 liner and insulated with TIR-300 asbestos-polyisoprene. A stress relief boot assembly is contained in the forward end of the motor case (Fig. 1a). A flange on the motor cylindrical section provides for attachment to the IMP spacecraft.

The contoured nozzle assembly contains a Graph-I-Tite G-90 carbon throat insert pinned and bonded to the nozzle adapter flange. The expansion cone is constructed of vitreous silica phenolic, externally coated with vapor-deposited aluminum. The cone is threaded, bonded, and pinned to the aluminum nozzle adapter flange. The nozzle assembly has a nominal 49.1:1 area ratio and a 14-deg half-angle at the exit plane. A styrofoam closure was bonded in the nozzle expansion cone. The closure was punctured prior to testing so that the rocket motor chamber pressure was equal to the simulated altitude pressure at motor ignition.

The TE-M-521-5 rocket motor contains a composite propellant grain formulation designated TP-H-3062 (ICC Class B), cast in an eight-point-star configuration. The isentropic exponent of the propellant exhaust gases is 1.18 (assuming frozen equilibrium).

Ignition was accomplished by two TE-P-386-7 pyrogen igniters (Fig. 1a) which incorporated Horex 4496 initiators and contained 20 BKNO<sub>3</sub> pellets (size 2A) used to initiate the 0.08-lbm primary polysulphide igniter grain. Nominal ignition current was 4.5 amp for 25 msec for each of the two igniters.

## 2.2 INSTALLATION

The motor assembly was cantilever mounted from the spindle face of a spin-fixture assembly in Propulsion Development Test Cell (T-3). The spin assembly was mounted on a thrust cradle, which was supported from the cradle support stand by three vertical and two horizontal double-flexure columns (Fig. 2). The spin-fixture assembly consists of a 10-hp squirrel-cage-type drive motor, a thrust bearing assembly, a 46-in.-long spindle having a 36-in.-diam aft spindle face, and a 170-channel slip-ring assembly. The spin fixture was rotated counterclockwise, looking upstream. Electrical leads to and from the igniters, pressure transducers, and thermocouples on the rotating motor were provided through a 170-channel, slip-ring assembly mounted between the forward and aft bearing assemblies of the spindle. Axial thrust was transmitted through the spindle-thrust bearing assembly to two double-bridge load cells mounted just forward of the thrust bearing on the motor axial centerline.

Preignition pressure altitude conditions were maintained in the test cell by a steam ejector operating in series with the ETF exhaust gas compressors. During the motor firing, the motor exhaust gases were used as the driving gas for the 29-in.-diam, ejector-diffuser system to maintain test cell pressure at an acceptable level.

## 2.3 INSTRUMENTATION

Instrumentation was provided to measure axial force, motor chamber pressure, lateral (nonaxial) force, test cell pressure, motor case and nozzle temperatures, motor rotational speed, and heat flux from the rocket plume. Table I (Appendix II) presents instrument ranges, recording methods, and measurement uncertainty for all reported parameters.

The axial force measuring system consisted of two double-bridge, strain-gage-type load cells mounted in the axial double-flexure column forward of the thrust bearing on the spacecraft centerline. The lateral (nonaxial) force measuring system consisted of two double-bridge, strain-gage-type load cells installed forward and aft between the flexure-mounted cradle and the cradle support stand normal to the rocket motor axial centerline and in the horizontal plane passing through the motor axial centerline (Fig. 2c).

Unbonded strain-gage-type transducers (0- to 1-psia) were used to measure test cell pressure. Bonded strain-gage-type transducers with ranges from 0 to 50 and 0 to 1000 psi were used to measure motor chamber pressure. Chromel<sup>®</sup>-Alumel<sup>®</sup> (CA) thermocouples were bonded to the motor case and nozzle (Fig. 3) to measure surface temperatures during and after motor burn time. Rotational speed of the motor-spacecraft assembly was determined from the output of a magnetic pickup. The heat flux from the rocket plume was measured by one calorimeter and five radiometers mounted as shown in Fig. 4.

The output signal of each measuring device was recorded on independent instrumentation channels. Primary data were obtained from four axial-thrust channels, three test cell pressure channels, and three motor chamber pressure channels. These data were recorded as follows: Each instrument output signal was indicated in totalized digital form on a visual readout of a millivolt-to-frequency converter. A magnetic tape system, recording in frequency form, stored the signal from the converter for reduction at a later time by an electronic computer. The computer provided a tabulation of average absolute values for each 0.10-sec time increment and total integrals over the cumulative time increments.

The output signal from the magnetic rotational speed pickup was recorded in the following manner: A frequency-to-analog converter was triggered by the pulse output from the magnetic pickup and in turn supplied a square wave of constant amplitude to the electronic counter, magnetic tape, and oscillograph recorders. The scan sequence of the electronic counter was adjusted so that it displayed directly the motor spin rate in revolutions per minute.

The millivolt outputs of the lateral (nonaxial) force load cells, radiometers, calorimeter, and thermocouples were recorded on magnetic tape from a multi-input, analog-to-digital converter and reduced to engineering units by an electronic computer.

A recording oscillograph was used to provide an independent backup of all operating instrumentation channels except the temperature and radiation measurement systems. Selected channels of thrust and pressures were recorded on null-balance, potentiometer-type strip charts for analysis immediately after a motor firing. Visual observation of the firing was provided by a closed-circuit television monitor. High-speed, motion-picture cameras provided a permanent visual record of the firing.

## 2.4 CALIBRATION

The thrust system calibrator weights, thrust load cells, and pressure transducers were laboratory calibrated prior to usage in this test. After installation of the measuring devices in the test cell, the thrust load cells were again calibrated at sea-level, nonspin ambient conditions and also at simulated altitude while spinning at 46 rpm.

The pressure recording systems were calibrated by an electrical, four-step calibration, using resistances in the transducer circuits to simulate selected pressure levels. The axial thrust instrumentation systems were calibrated by applying to the thrust cradle known forces, which were produced by deadweights acting through a bell crank. The calibrator is hydraulically actuated and remotely operated from the control room. Thermocouple recording instruments were calibrated by using known millivolt levels to simulate thermocouple outputs. Calibration curves for the radiometers and the calorimeter were supplied by the transducer manufacturer.

After the motor firing, with the test cell still at simulated altitude pressure, the recording systems were recalibrated to determine any shift.

Calibrations of the lateral (nonaxial) forces measuring system were conducted using the procedure outlined in Ref. 6.

### SECTION III PROCEDURE

The TCC TE-M-521-5 rocket motor (S/N PV32-248-2) and associated hardware arrived at AEDC on July 10, 1972. The motor was visually inspected for possible shipping damage and radiographically inspected for grain cracks, voids, or separations and found to meet criteria provided by the manufacturer.

After radiographic inspection, the motor was stored in an area temperature conditioned at  $70 \pm 5^{\circ}\text{F}$ , where the motor was checked to ensure correct fit of mating hardware, the electrical resistances of the igniters were measured, and the nozzle exit diameter was obtained. The motor was leak checked after installation of the chamber pressure transducers. The entire assembly was weighed and photographed. Thermocouples had been bonded to the nozzle and motor case at the manufacturer's facilities. After the thrust adapter was secured to the motor case, the assembly was mounted on a spin table, and radial dimensions of the spacecraft flange and nozzle flange as a function of angular position relative to the centerline of the assembly were determined to facilitate alignment with the spin-rig spin axis during test cell installation.

After installation of the assembly in the test cell, the motor centerline was axially aligned with the spin-rig spin axis by rotating the motor assembly and measuring the deflection of the nozzle flange and the motor flange with a dial indicator and making appropriate adjustments. The instrumentation connections were made, and the motor assembly was balanced at a rotational speed of 46 rpm. Cell temperature was controlled to condition the motor assembly at  $40^{\circ}\text{F}$  for a period in excess of 24 hr. A continuity check of all electrical systems was performed, prefire ambient calibrations were completed, the test cell pressure was reduced to the desired simulated altitude, and spinning of the unit was started. After spinning had stabilized at 46 rpm, a complete set of altitude calibrations was taken.

The final operation prior to firing the motor was to adjust the firing circuit resistance to provide the desired current to the igniter squibs. The entire instrumentation measuring-recording complex was activated, and the motor was fired while spinning (under power) at 46 rpm.

Spinning of the motor was continued for approximately 70 min after burnout, during which time motor and blanket temperatures were recorded, and postfire calibrations were accomplished. The unit was decelerated slowly until rotation had stopped, and another set of calibrations was taken. The test cell pressure was then returned to ambient conditions, and the motor assembly was inspected, photographed, and removed to the storage area. Postfire inspections at the storage area consisted of measuring the throat and exit diameters of the nozzle, weighing the motor, and photographically recording the postfire condition of the motor.

## SECTION IV RESULTS AND DISCUSSION

One Thiokol Chemical Corporation TE-M-521-5 solid-propellant rocket motor (S/N PV32-248-2) was successfully fired at an average altitude of 108,000 ft. The motor was prefire vibration conditioned, and temperature conditioned at  $40 \pm 5^\circ\text{F}$  for a period in excess of 24 hr prior to firing with the motor assembly spinning about the motor longitudinal axis at 46 rpm. The general objective of this quality assurance program was to verify compliance of motor performance with the manufacturer's specifications (Ref. 5). Specific primary objectives were to determine vacuum ballistic performance, altitude ignition characteristics, motor structural integrity, and test article temperature-time histories during and after motor operation. Additional secondary objectives were to measure the motor lateral (nonaxial) thrust component during motor operation and to measure radiation heat flux in the vicinity of the nozzle exit plane. The resulting data are presented in both tabular and graphical form.

Motor performance based on action time ( $t_a$ ) and total burn time ( $t_{is}$ ) is summarized and compared with results from previous altitude firings of the TE-M-521 in Table II. Motor physical dimensions are compared with the previous motors in Table III. Altitude ignition characteristics, rocket exhaust plume radiation heat flux, and temperature-time histories of motor case and nozzle are presented and discussed. When multiple channels of equal accuracy instrumentation were used to obtain values of a single parameter, the average values were used to calculate the data presented.

### 4.1 ALTITUDE IGNITION CHARACTERISTICS

The motor was ignited at a pressure altitude of 115,000 ft. The average simulated altitude during motor action time ( $t_a$ ) was 108,000 ft. An analog trace of thrust, chamber pressure, and test cell pressure characteristics during motor ignition are presented in Fig. 5.

Ignition time ( $t_i$ ) was 0.11 sec and was within the manufacturer's specifications of not less than 0.025 sec or greater than 0.250 sec for a temperature range of 0 to  $110^\circ\text{F}$ . Ignition lag time ( $t_l$ ) was 0.006 sec, utilizing both pyrogen igniters. The ignition lag time of motors previously tested at the AEDC which were temperature conditioned at  $40^\circ\text{F}$  were 0.002 sec (Ref. 2), utilizing two pyrogen igniters, and 0.006 sec (Ref. 3), and 0.008 sec (Ref. 4), utilizing two pyrogen igniters. One motor, temperature conditioned at  $100^\circ\text{F}$  and utilizing both pyrogen igniters had an ignition lag time of 0.002 sec (Ref. 3). Ignition lag times of all TE-M-521 motors tested at the AEDC were within the manufacturer's estimated value of  $0.006 \pm 0.005$  sec. No effect of prefire grain temperature or number of pyrogen igniters utilized is apparent on ignition lag time.

## 4.2 ALTITUDE BALLISTIC PERFORMANCE

Since the nozzle does not operate fully expanded at the low chamber pressures encountered during tailoff, the measured total impulse data during this period cannot be corrected to vacuum conditions by adding the product of cell pressure integral and nozzle exit area. Therefore, total burn time and action time were segmented, and the method used to determine vacuum impulse is illustrated in Fig. 6. The time of exhaust nozzle flow breakdown ( $t_{bd}$ ) was considered to have occurred simultaneously with the exhaust diffuser flow breakdown (as indicated by a rapid increase in cell pressure during tailoff). The flow at the nozzle throat was considered sonic velocity until the time ( $t_{is}$ ) at which the ratio of chamber-to-cell pressure had decreased to a value of 1.3. The time interval ( $t_1$  to  $t_2$ ) is a one-second interval of motor operation just prior to decrease in chamber pressure (Fig. 6).

Performance characteristics of the motor reported herein and the four previously fired TE-M-521 motors (Refs. 2, 3, and 4) are presented in Table II. Action time ( $t_a$ ) for motor S/N PV32-248-2 was 20.68 sec, which was 0.56 sec less than that for the Ref. 2 motor, which was fired at the same spin rate (46 rpm), and at the same temperature (40°F) as the motor reported herein. The total burn time ( $t_{is}$ ) for motor S/N PV32-248-2 was 21.63 sec or 5.84 sec less than the Ref. 2 motor. Vacuum total impulse was 71,469 lbf-sec for motor S/N PV32-248-2 and 71,671 lbf-sec for Ref. 2 motor; both motors were within the manufacturer's specifications of  $71,350 \pm 350$  lbf-sec,  $3\sigma$  deviation. Vacuum specific impulse (based on  $t_{is}$  and the manufacturer's stated propellant weight) was 289.08 lbf-sec/lbm for motor S/N PV32-248-2 and 289.81 lbf-sec/lbm for the Ref. 2 motor. Vacuum specific impulse based on expended mass, as determined by pre- and post-fire motor weight measurements taken at the AEDC, was 288.76 lbf-sec/lbm for the motor reported herein, compared with 286.83 lbf-sec/lbm for the Ref. 2 motor.

It was noted (Table III) that the expended mass from the motor reported herein was approximately equal to the manufacturer's stated propellant weight, whereas, for the previous four motor firings (Ref. 2 to 4), expended mass was 2 to 3 lbm greater than the manufacturer's stated propellant weight. Postfire inspection of the motor case at the AEDC revealed appreciable unburned propellant remaining in the motor case (8 slivers, each approximately 12 in. long and from 1/2 to 3/4 in. wide). This unburned propellant could account for the shorter total burn time of the motor firing reported herein (21.63 sec), as compared with the total burn time (27.47 sec) of the Ref. 2 motor. However, the vacuum specific impulse performance of the current motor (288.76 lbf-sec/lbm, based on expended mass) was almost 0.7 percent greater than the Ref. 2 motor. The improvement in performance was further evidenced by the approximate 1-percent increase in vacuum thrust coefficient. The reason for the improvement in ballistic performance has not been determined.

A comparison of thrust and chamber pressure is presented in Fig. 7 for motors fired with the same prefire temperature conditioning (40°F) but with spin rates of 46 rpm (current test and Ref. 2) and 100 rpm (Ref. 3). The thrust and chamber pressure data from the current test are approximately 1.5 percent higher than data from the Ref. 2 and 3 tests, but had a burn time ( $t_b$ ) 3 percent shorter. The vacuum total impulse of 71,469 lbf-sec, from the current test, is 0.28 percent lower than the value measured during the previous test (Ref. 2); however, the vacuum total impulse for both motors is within the manufacturer's specifications.

#### 4.3 STRUCTURAL INTEGRITY AND MOTOR TEMPERATURE-TIME HISTORY

External postfire examination of the motor case and nozzle assembly did not reveal any evidence of thermal damage (Fig. 8). The pinned nozzle throat section was securely in place after the test. Nozzle throat measurements indicated a throat area increase of 10.5 percent from the prefire area. The nozzle exit area had decreased approximately 1.02 percent from the prefire area.

Motor case and nozzle temperature variations with time are presented in Fig. 9. The maximum indicated case temperature (590°F) occurred approximately 450 sec after motor ignition, as indicated by the thermocouple (TC-14) located on the motor case near the nozzle closure (Fig. 9f) and was within the maximum manufacturer's limit of 600°F. The maximum case temperature recorded during the Ref. 2 motor test was 525°F, 600 sec after motor ignition. The maximum indicated nozzle temperature (560°F) occurred 150 sec after motor ignition, as indicated by the thermocouple (TN-12) located near the nozzle throat (Fig. 9f); the previous maximum nozzle temperature for Ref. 2 motor was 705°F, 245 sec after motor ignition. The Ref. 2 motor was enclosed in a flightweight thermal insulation blanket.

#### 4.4 PLUME RADIATION

Five narrow-angle radiometers were used to obtain rocket exhaust plume radiation heat flux data. One wide-angle calorimeter was used to obtain background radiation. The instruments were positioned around the nozzle assembly as shown in Fig. 4.

The variation of radiation heat flux with time is presented in Fig. 10. The maximum radiation heat flux (prior to motor burnout and diffuser breakdown) was 18 Btu/ft<sup>2</sup>-sec (Fig. 10f, R-5) and occurred 19 sec after ignition. The maximum measured radiation was 3 Btu/ft<sup>2</sup>-sec higher than the maximum measured during the previous test (Ref. 2). Measured radiation heat flux increased throughout the firing.

#### 4.5 LATERAL (NONAXIAL) THRUST VECTOR MEASUREMENT

An additional objective for this test was to measure the lateral (nonaxial) component of motor thrust. The recorded lateral thrust data were corrected for installation and/or electronic effects as described in Ref. 6.

The maximum magnitude of lateral thrust recorded during the near steady-state portion of motor operation was 2.9 lbf and occurred at approximately 2 and 14 sec after motor ignition (Fig. 11). The corresponding angular positions of the lateral thrust vector (measured clockwise looking upstream) were 50 and 45 deg.

## SECTION V SUMMARY OF RESULTS

One Thiokol Chemical Corporation TE-M-521-5 solid-propellant rocket motor was successfully fired at an average pressure altitude of about 108,000 ft, while spinning at 46 rpm about the motor axis. The motor was prefire vibration conditioned, and temperature conditioned in a controlled environment of  $40 \pm 5^\circ\text{F}$  for a period in excess of 24 hr prior to firing. Results are summarized as follows:

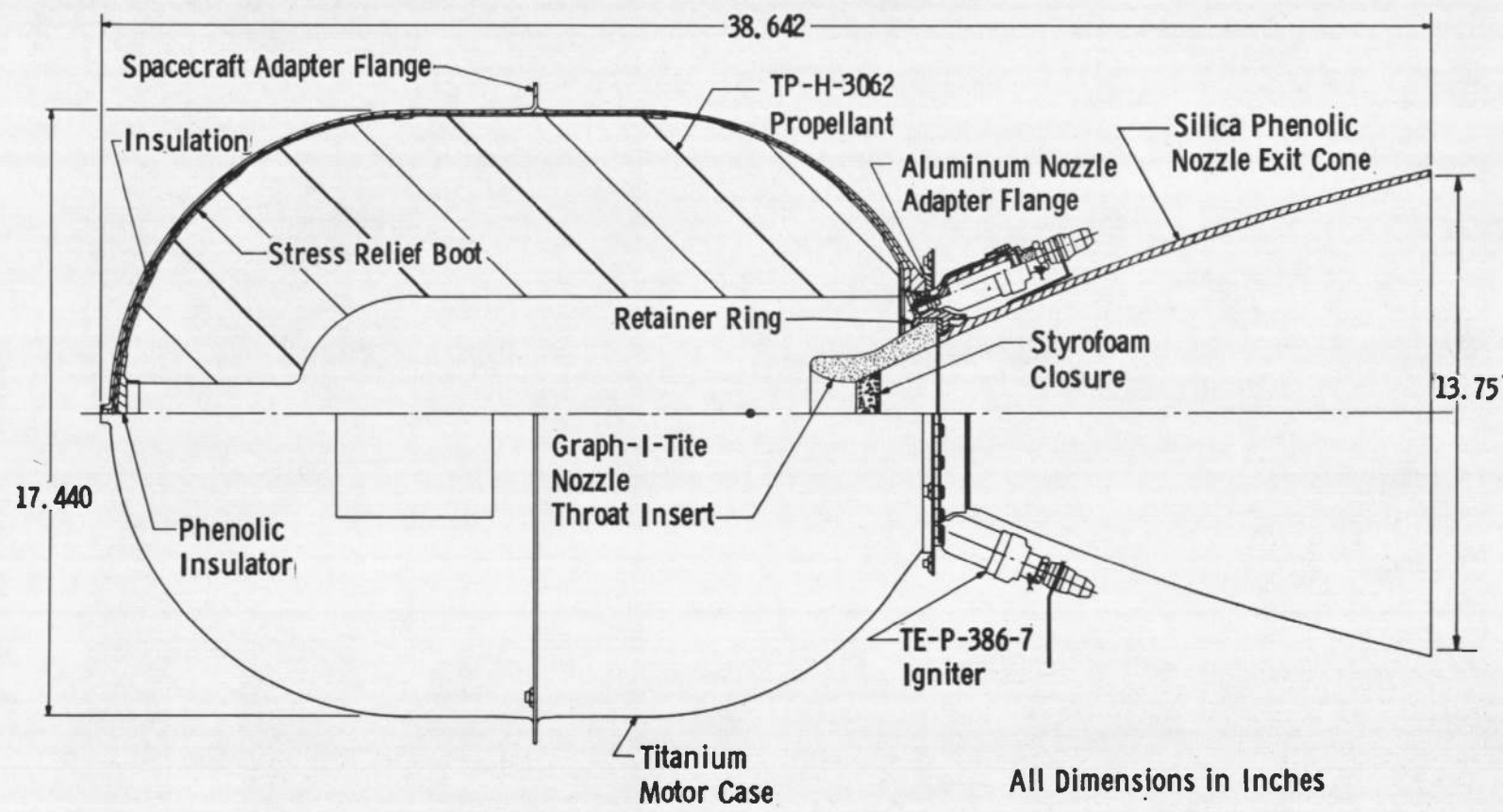
1. Ignition time ( $t_i$ ), the time interval from application of ignition voltage to attainment of 90 percent of peak thrust during the ignition transient, was 0.11 sec and met the manufacturer's specifications.
2. Ignition lag time ( $t_l$ ), the time interval from the time at which ignition voltage was applied to the igniter circuit to the first perceptible rise in chamber pressure, was 0.006 sec. Action time ( $t_a$ ), the time interval between 10 percent of maximum chamber pressure during ignition and 10 percent of maximum chamber pressure during tailoff, was 20.68 sec.
3. Total burn time ( $t_{is}$ ), the time interval between the application of ignition voltage to the time at which the ratio of chamber-to-cell pressure had decreased to 1.3 at tailoff, was 21.63 sec. This burn time was 5.84 sec less than the previous altitude firing of the TE-M-521-5 and is attributed to a faster propellant burn rate and incomplete propellant combustion. Eight slivers of propellant, approximately 12 in. long and 1/2 to 3/4 in. wide remained in the motor case.
4. Vacuum total impulse, based on  $t_{is}$ , was 71,469 lbf-sec, and was within the manufacturer's specification of  $71,350 \pm 350$  lbf-sec. Vacuum specific impulse, based on  $t_{is}$  and expended mass, was 288.76 lbf-sec/lbm, and was almost 0.7 percent greater than the previous TE-M-521-5 motor. The improvement in motor performance was further evidenced by an approximate 1-percent increase in vacuum thrust coefficient (1.856 for the current motor, compared with 1.838 for the previous -5 motor). The reason for the improved motor ballistic performance has not been determined.
5. The nozzle throat area increased approximately 10.5 percent from the prefire area during the firing. The nozzle exit area decreased nominally 1.02 percent.

6. The maximum motor case temperature was 590°F and occurred approximately 450 sec after motor ignition. The maximum nozzle temperature was 560°F and occurred approximately 150 sec after ignition.
7. The maximum magnitude of lateral (nonaxial) thrust measured during near steady-state portion of motor operation was 2.9 lbf and occurred at approximately 2 and 14 sec after first indication of chamber pressure.
8. The maximum radiation heat flux was 18 Btu/ft<sup>2</sup>-sec at the exit plane 19 sec after ignition and was within the range measured during previous tests. Measured radiation heat flux increased throughout the firing.

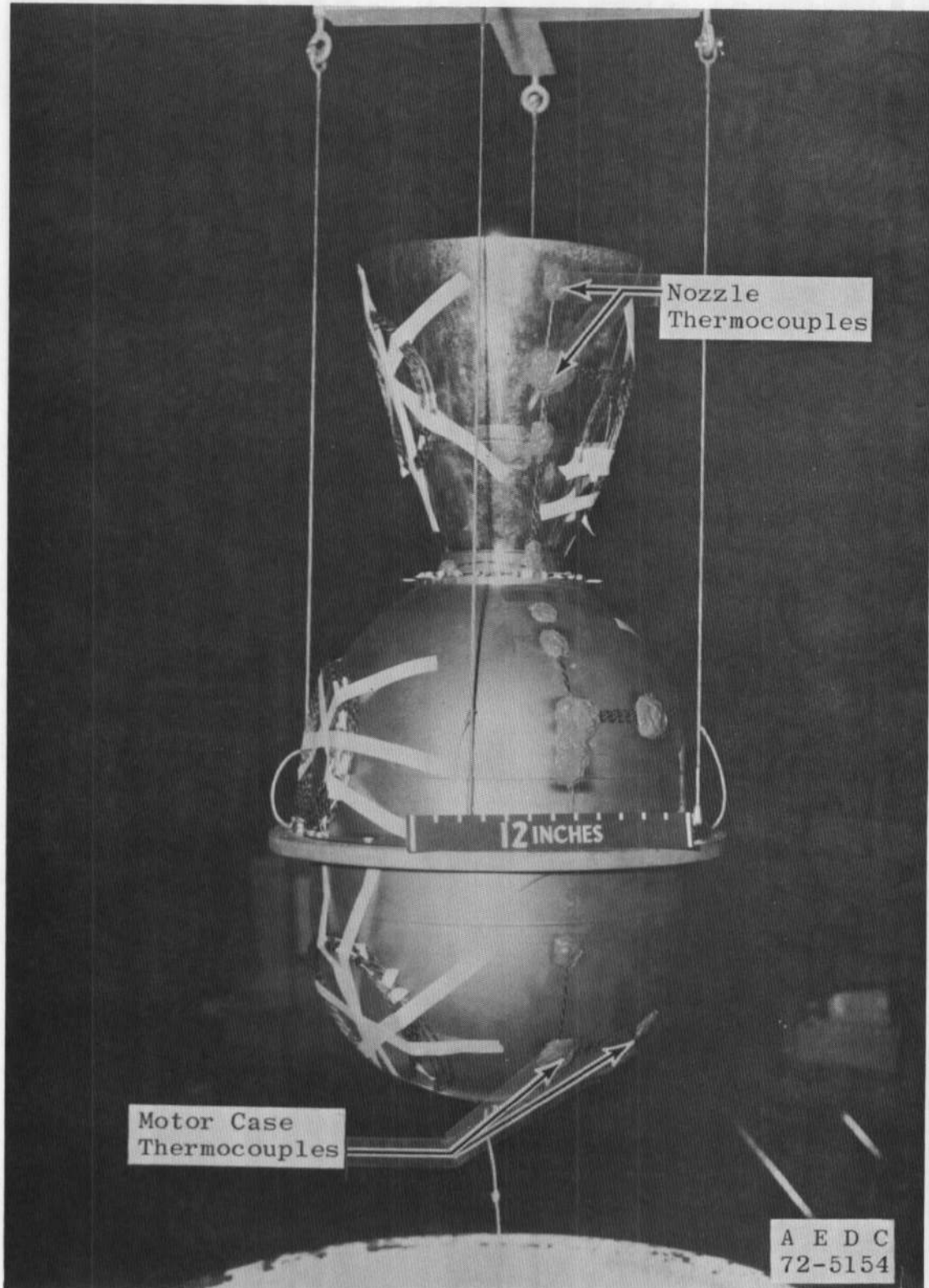
### REFERENCES

1. Blevins, Jay. "IMP Kick Motor Test Plan, Test 5205-101." Thiokol Chemical Corporation, Elkton, Maryland. September 1971.
2. Cimino, A. A. "Evaluation of the Thiokol TE-M-521-5 Apogee Kick Motor Tested in the Spin Mode at Simulated Altitude Conditions." AEDC-TR-72-85 (AD747081), August 1972.
3. Brooksbank, R. M. and Bahor, L. R. "Evaluation of Two IDCSP/A Spacecraft Apogee Kick Motors Tested in the Spin Mode at Simulated Altitude Conditions." AEDC-TR-68-250 (AD844673), December 1968.
4. Bahor, L. R. "Ballistic Performance of a Thiokol TE-M-521 IDCSP/A Spacecraft Apogee Kick Motor Tested in the Spin Mode at Simulated Altitude Conditions." AEDC-TR-69-155 (AD855512), July 1969.
5. NAS 7-801 Specifications. "TE-M-521-5 Apogee Motor." GSFC TCN 470-18475, April 13, 1971.
6. Nelius, M. A. and Harris, J. E. "Measurements of Nonaxial Forces Produced by Solid-Propellant Rocket Motors Using a Spin Technique." AEDC-TR-65-228 (AD474410), November 1965.

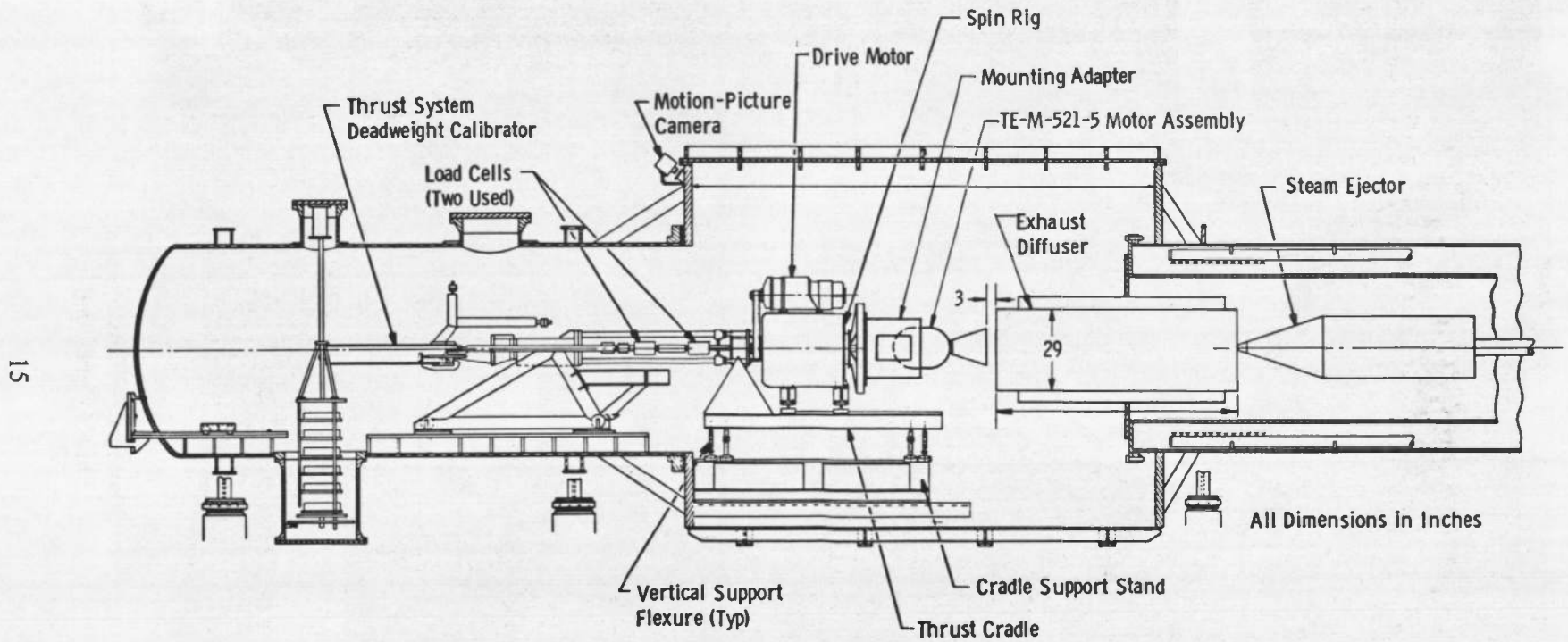
**APPENDIXES**  
**I. ILLUSTRATIONS**  
**II. TABLES**



a. Schematic  
Fig. 1 Thiokol Chemical Corporation TE-M-521-5 Solid-Propellant Rocket Motor

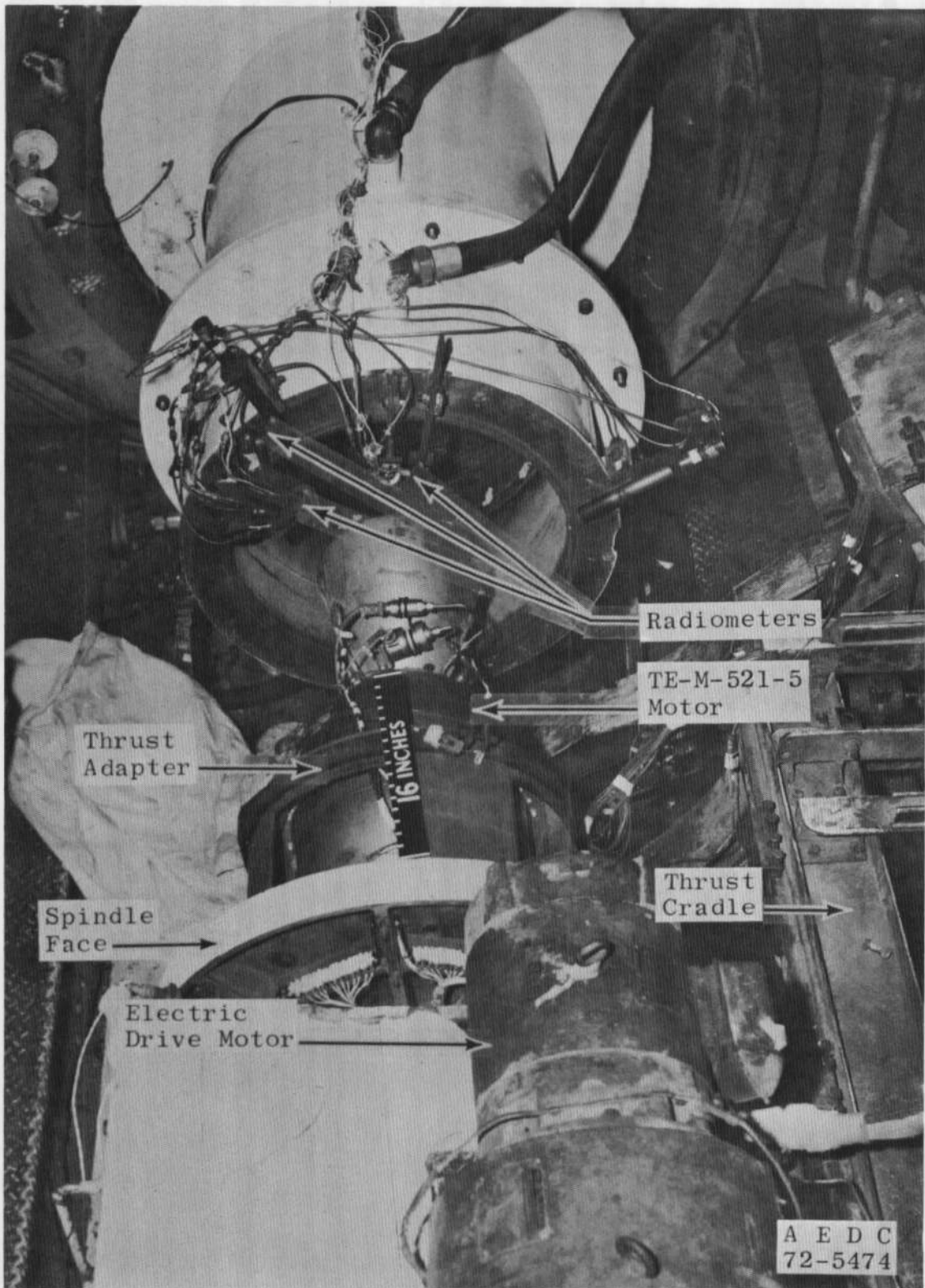


b. Photograph (Less Igniters)  
Fig. 1 Concluded

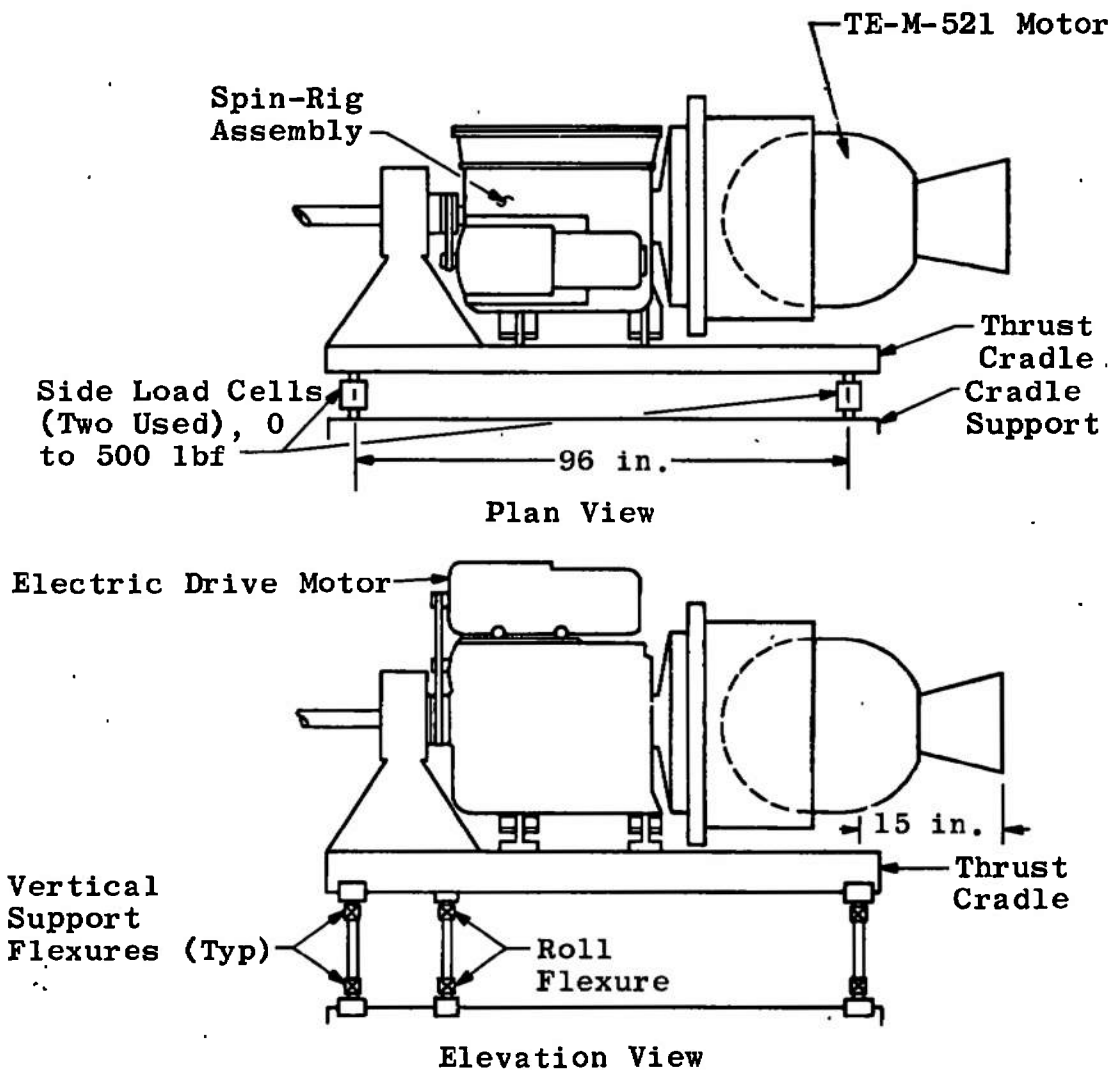


a. Schematic

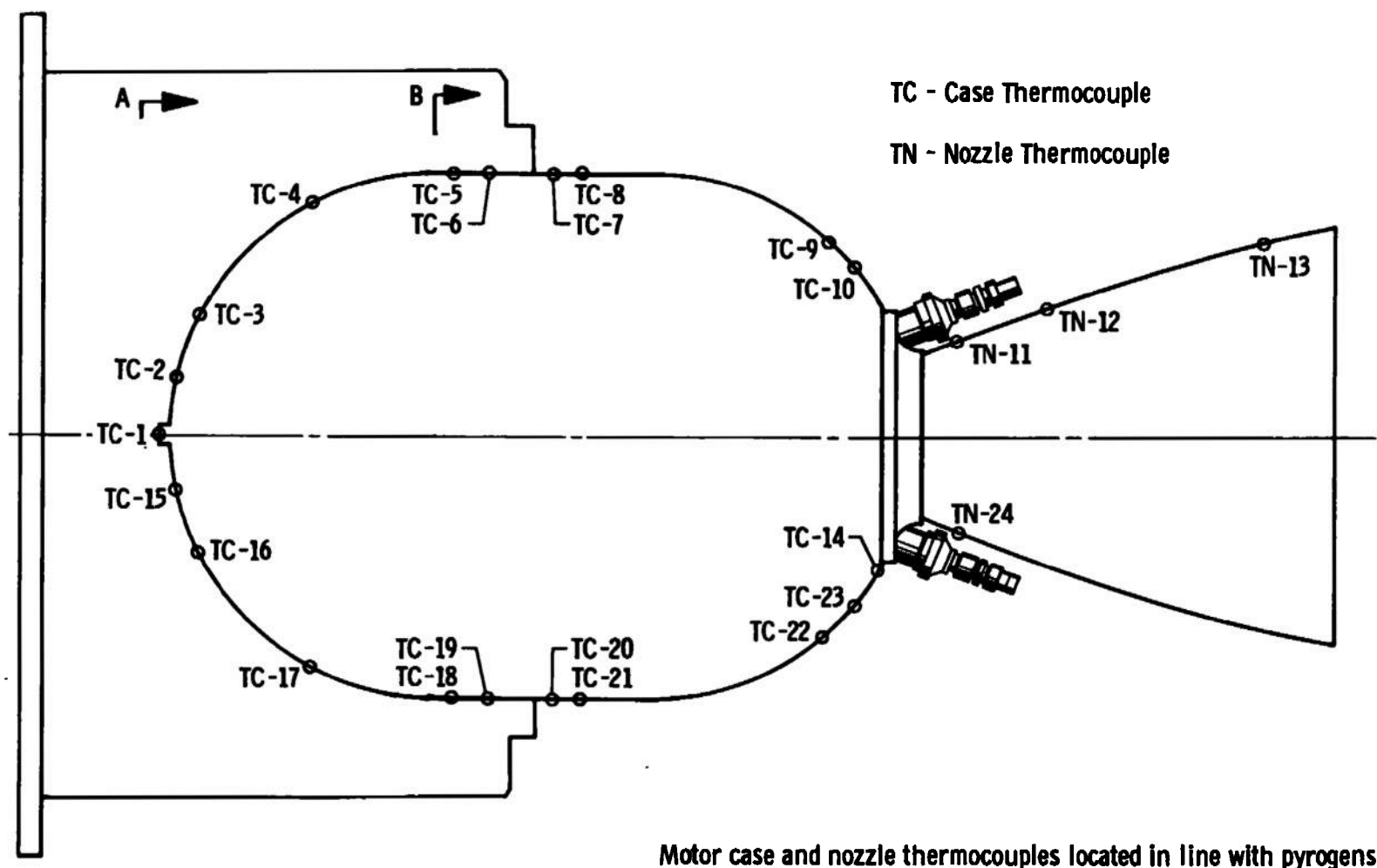
Fig. 2 Installation of the Thiokol TE-M-521-5 Rocket Motor in Propulsion Development Test Cell (T-3)



b. Photograph  
Fig. 2 Continued



c. Details of Nonaxial Force Measuring System  
 Fig. 2 Concluded



18

Fig. 3 Schematic of Motor Showing Thermocouple Locations

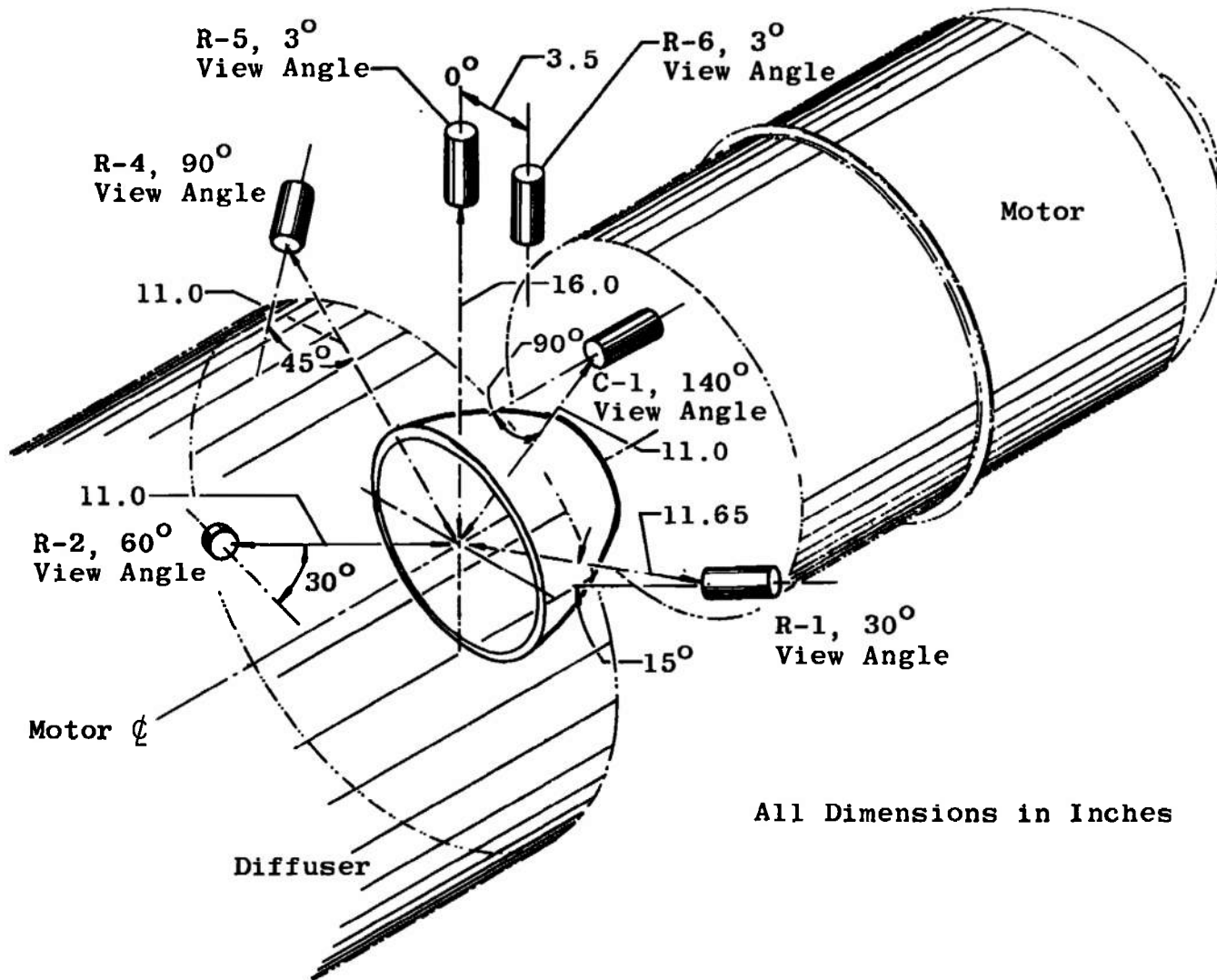


Fig. 4 Schematic of Motor Installation Showing Radiometer and Calorimeter Locations

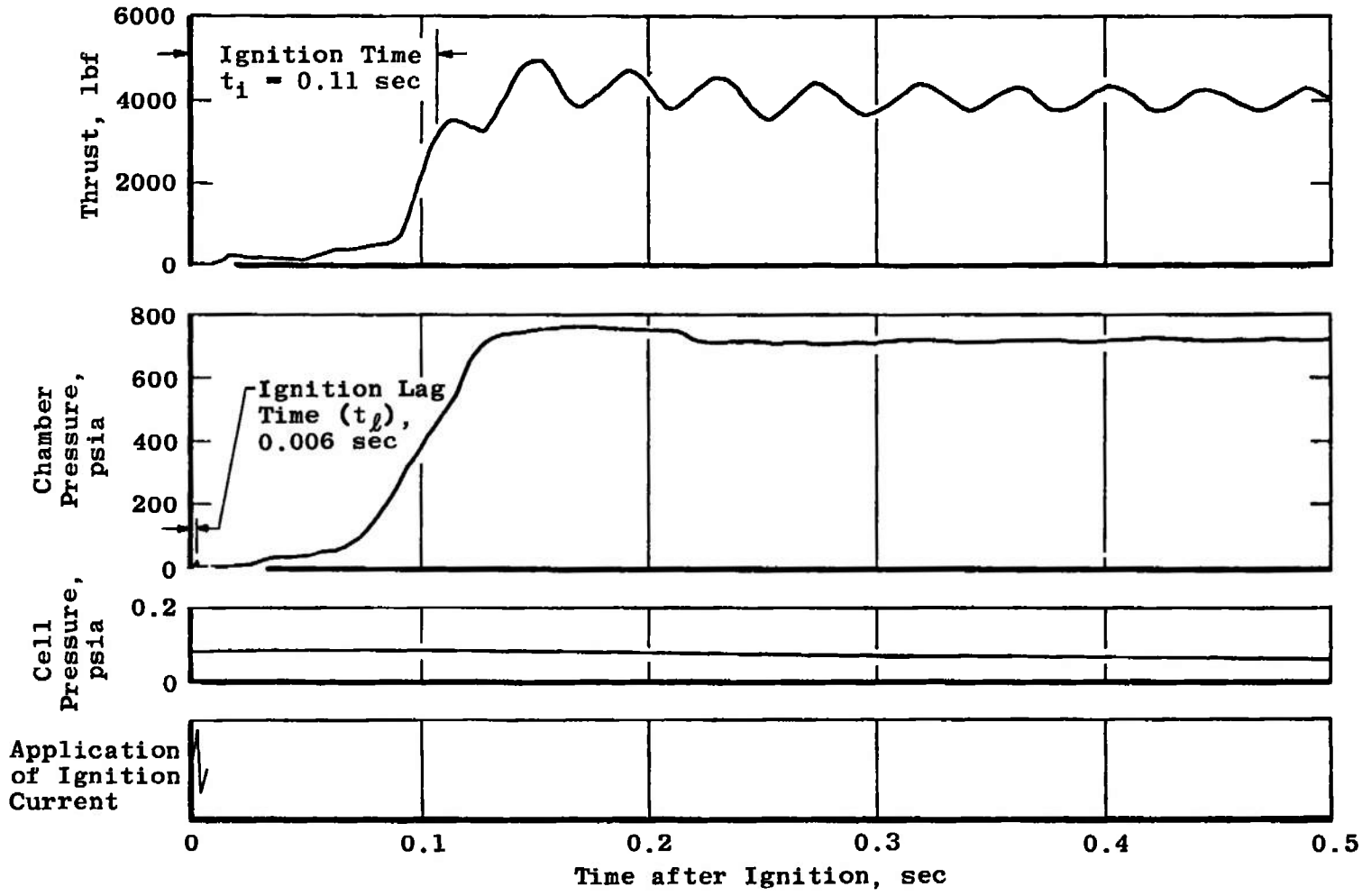
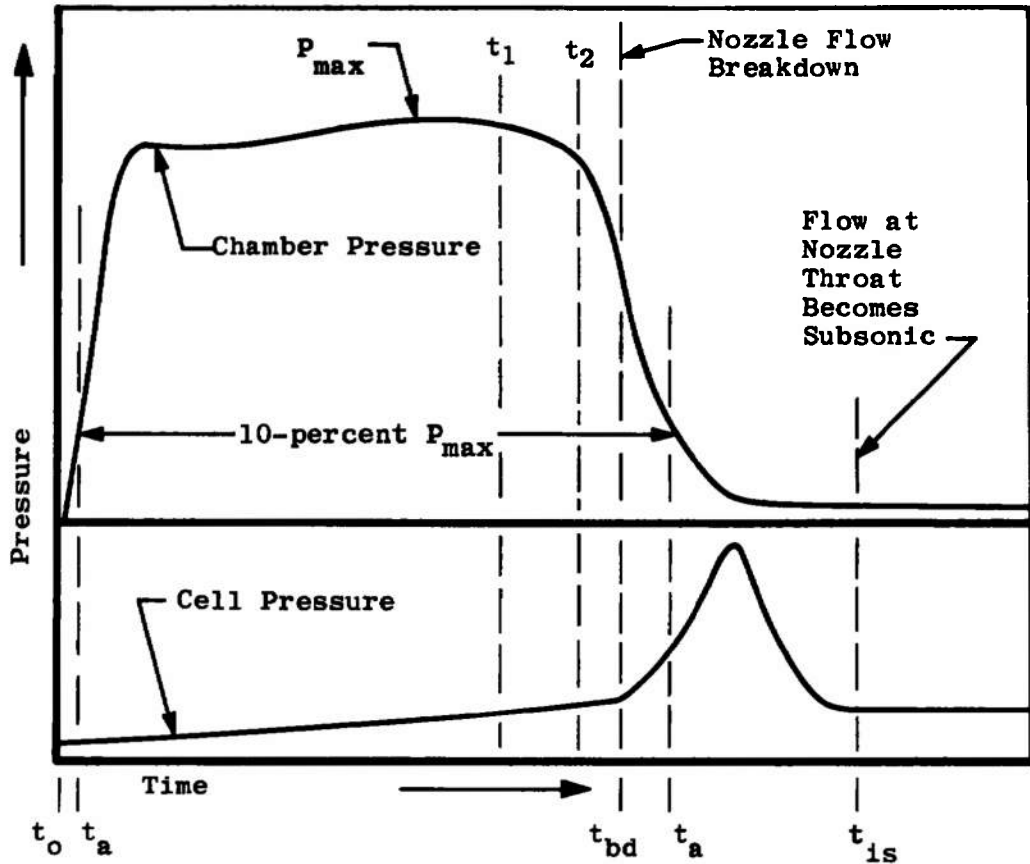


Fig. 5 Analog Trace of Motor Ignition Event



$$I_{vac\_total} = \int_{t_0}^{t_{bd}} F dt + A_{ex(avg)} \int_{t_0}^{t_{bd}} P_{cell} dt + \bar{c}_f A_{th(post)} \int_{t_{bd}}^{t_{is}} P_{ch} dt$$

$$I_{vac\_action} = \int_{t_{a\,ignition}}^{t_{bd}} F dt + A_{ex(avg)} \int_{t_{a\,ignition}}^{t_{bd}} P_{cell} dt + \bar{c}_f A_{th(post)} \int_{t_{bd}}^{t_{a\,tailoff}} P_{ch} dt$$

where:  $\bar{c}_f = \frac{\int_{t_1}^{t_2} F dt + A_{ex,post} \int_{t_1}^{t_2} P_{cell} dt}{A_{t,post} \int_{t_1}^{t_2} P_{ch} dt}$

established from data during the time interval from 18.00 ( $t_1$ ) to 19.00 ( $t_2$ ) sec after first indication of chamber pressure.

Fig. 6 Definition of Vacuum Total and Action Impulse

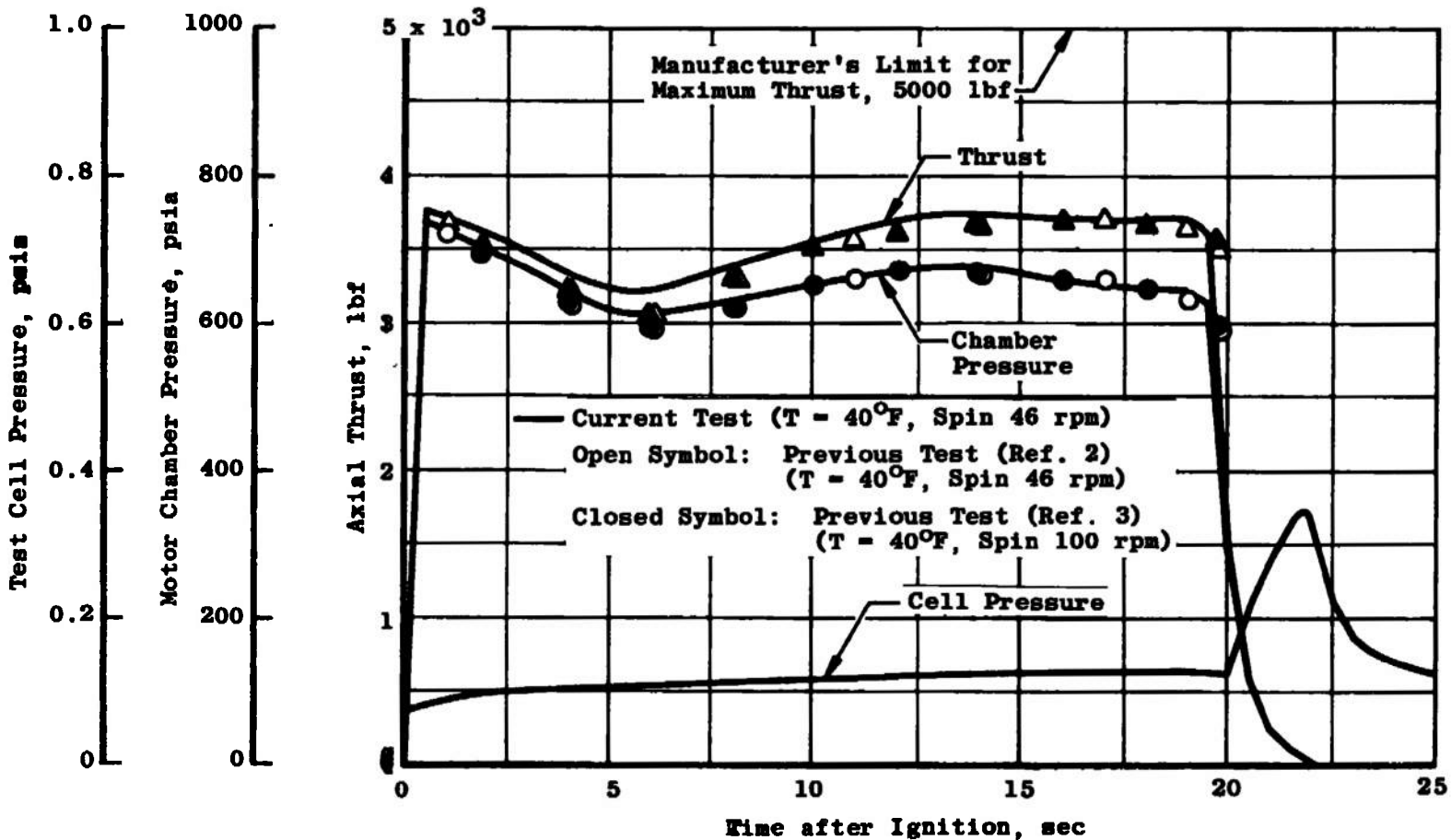
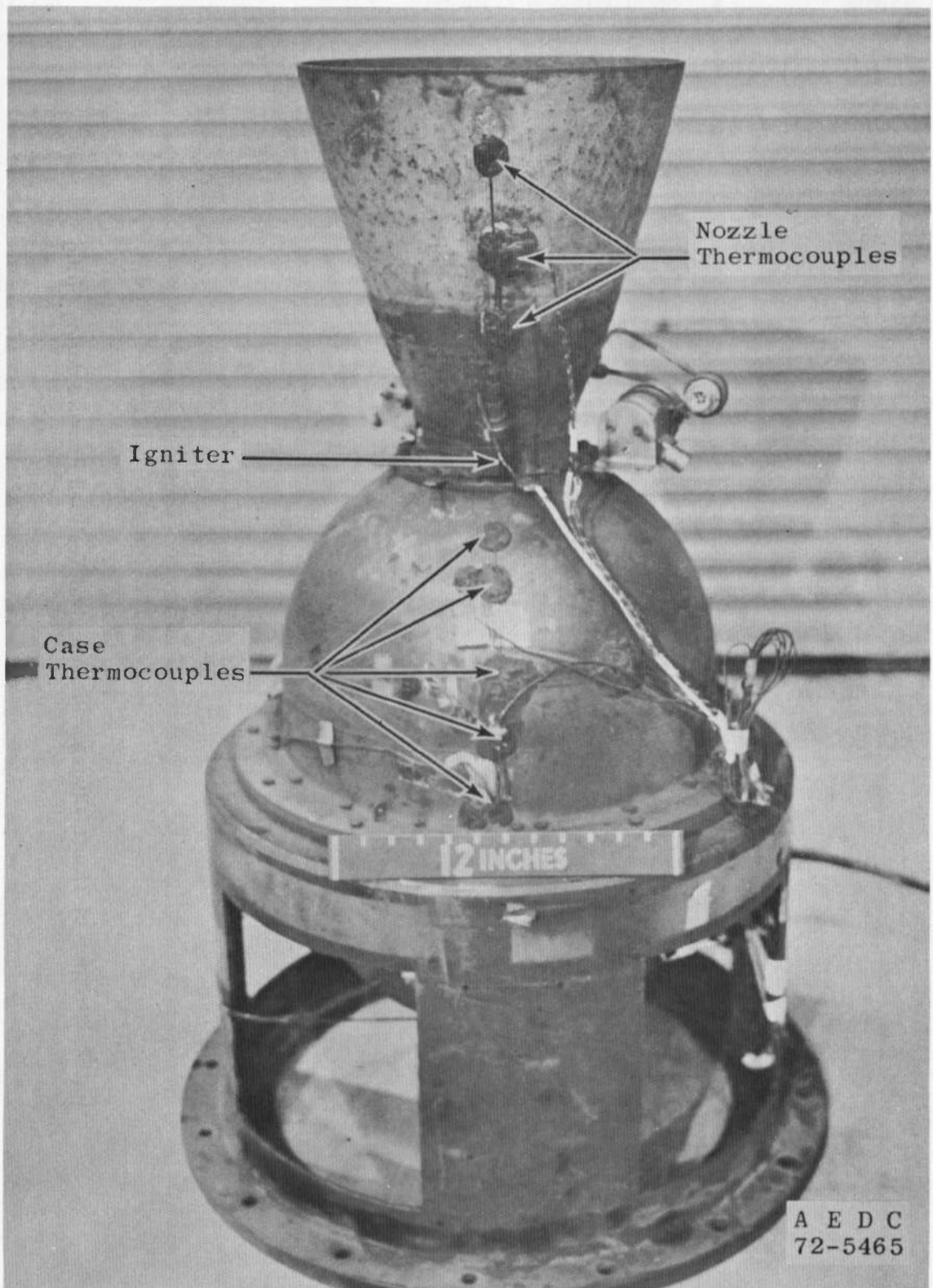
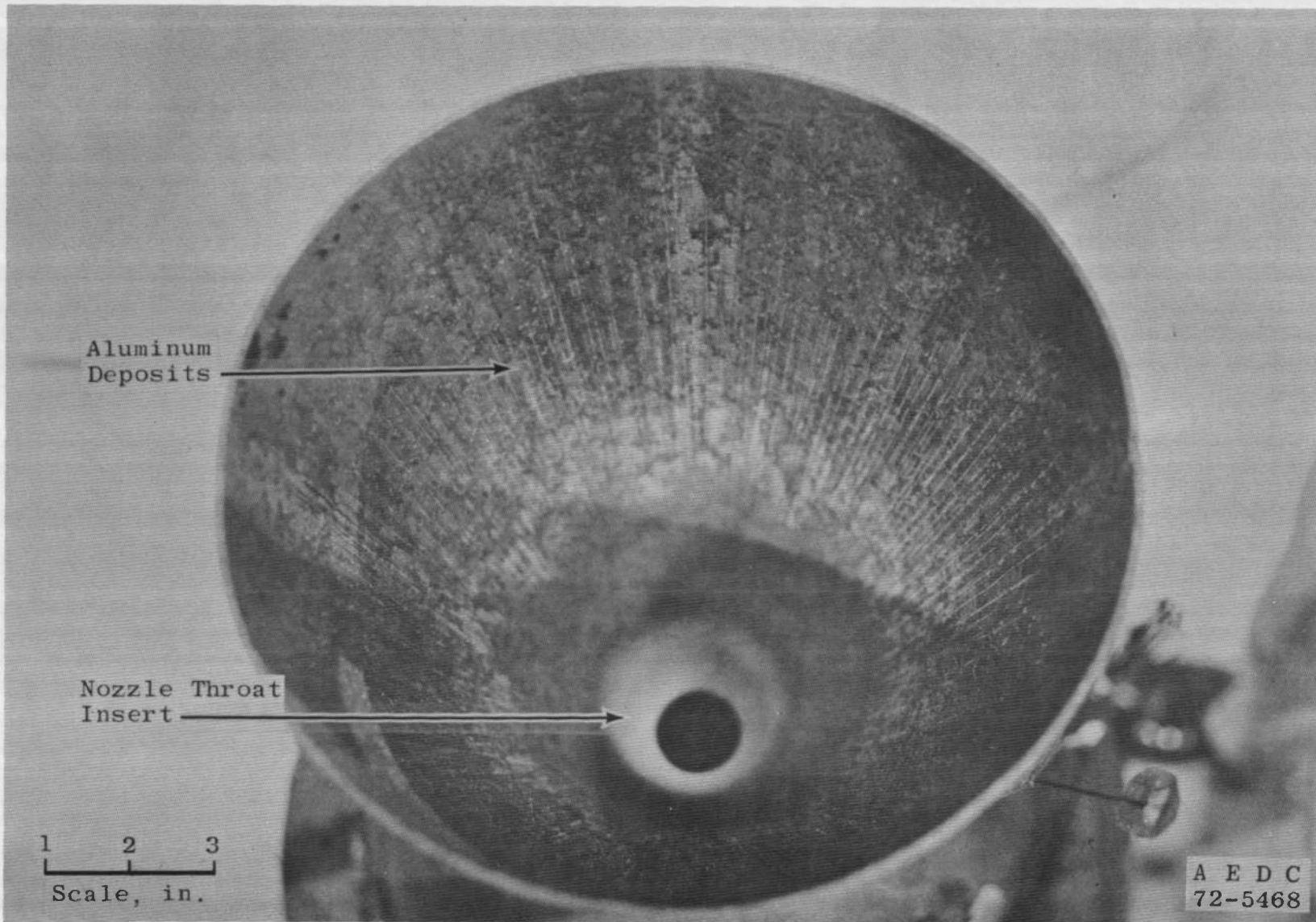


Fig. 7 Variation of Thrust, Chamber Pressure, and Test Cell Pressure during Firing

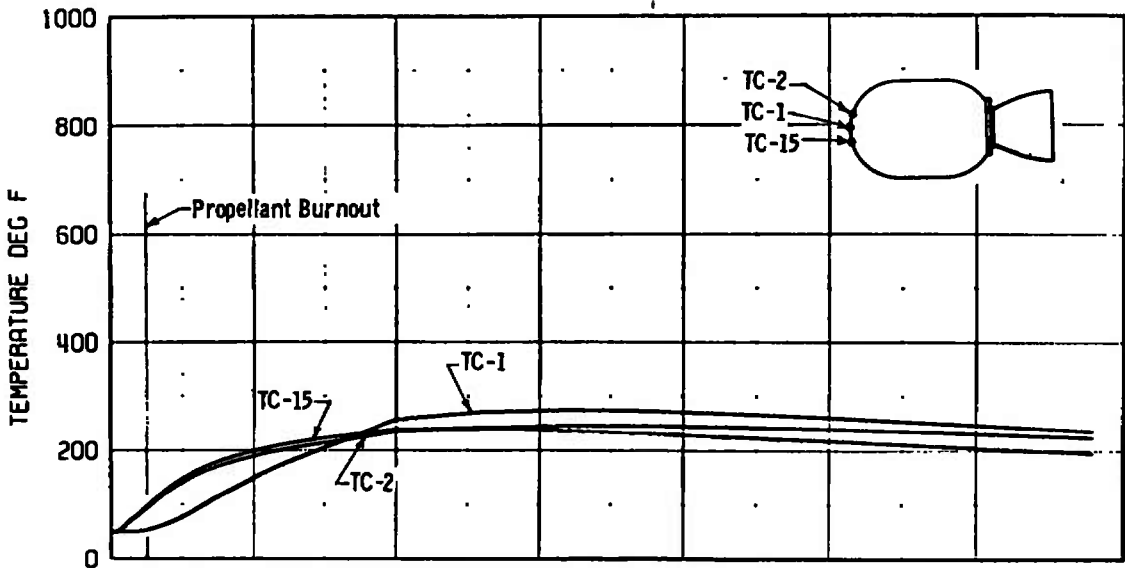


a. Motor Case and Nozzle  
Fig. 8 Postfire Photographs of Motor Assembly

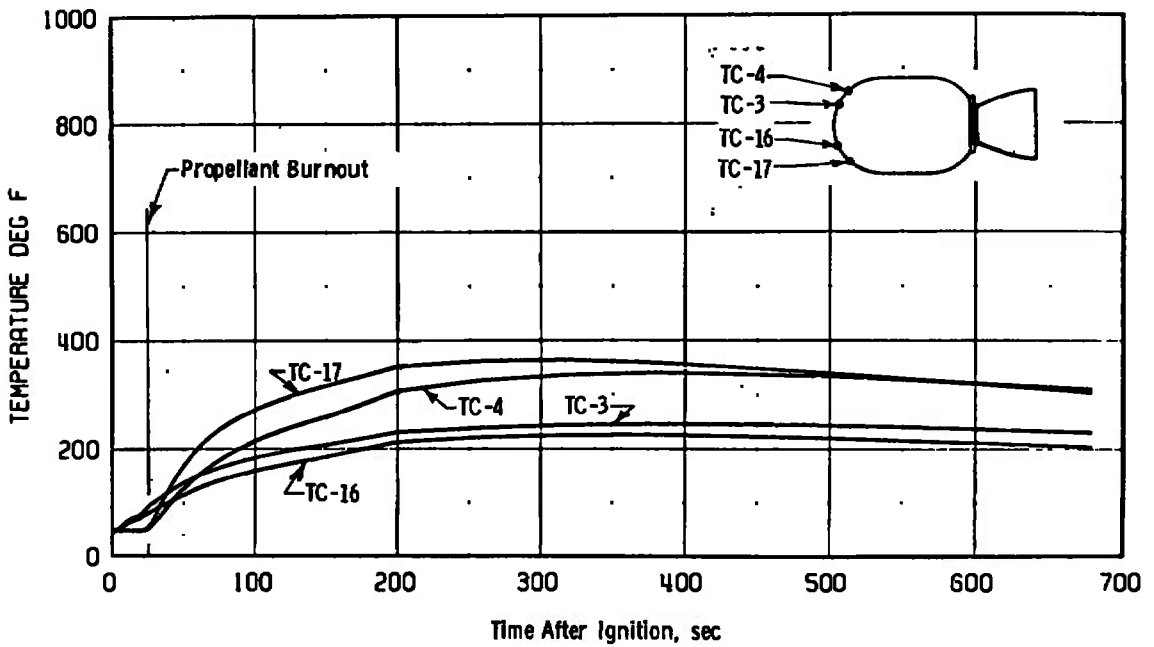


24

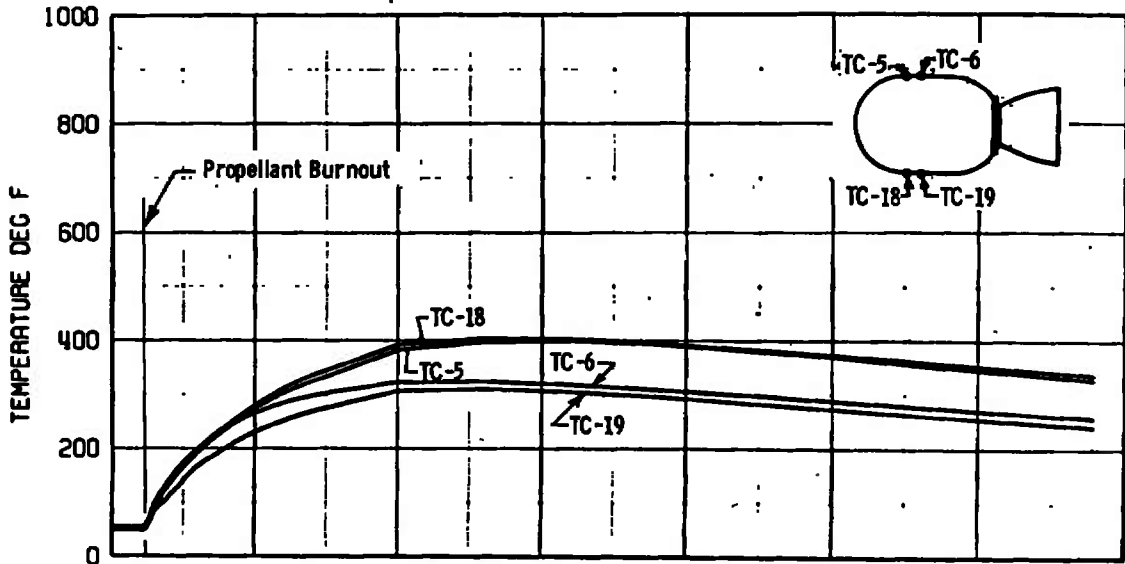
b. Nozzle  
Fig. 8 Concluded



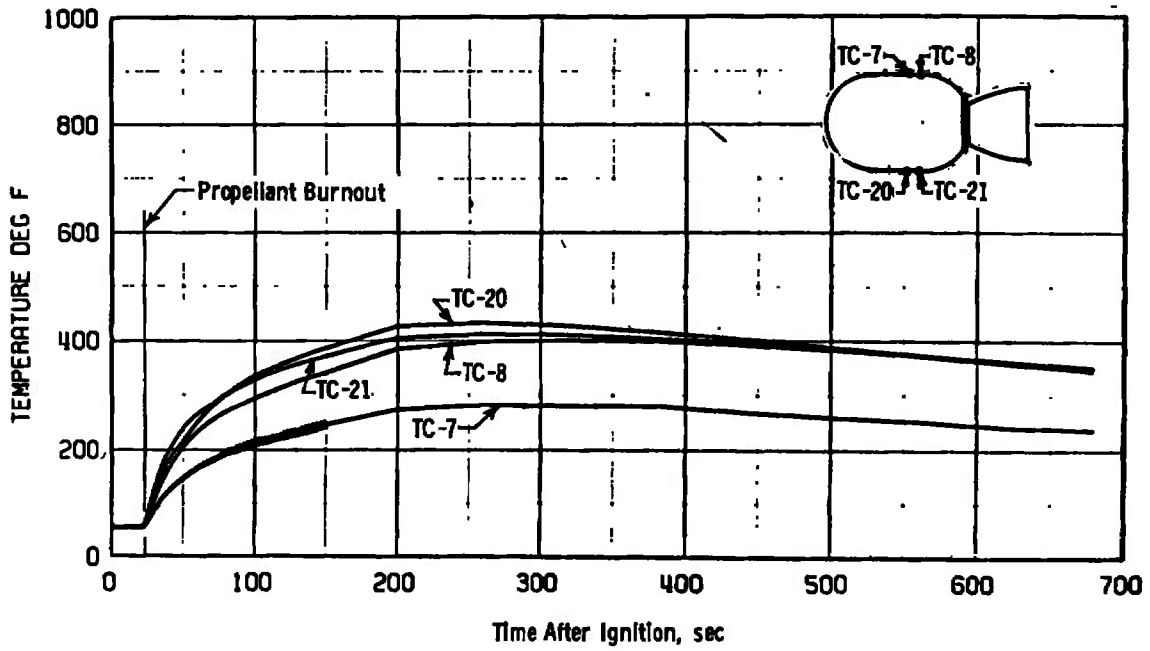
a. Motor Case; TC-1, TC-2, and TC-15



b. Motor Case; TC-3, TC-4, TC-16, and TC-17  
 Fig. 9 Motor Temperature Variation with Time

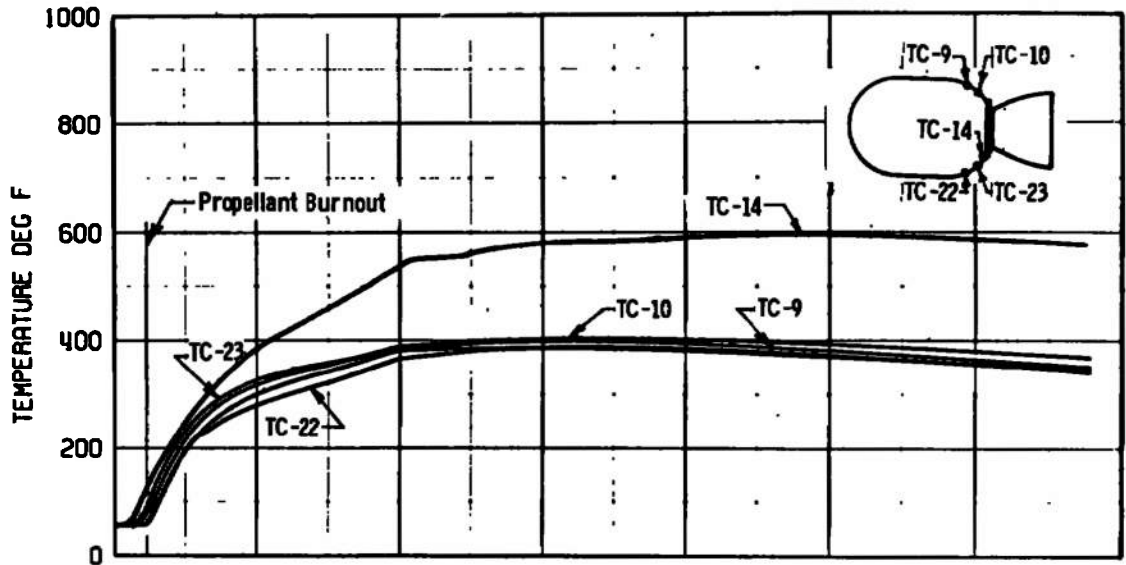


c. Motor Case; TC-5, TC-6, TC-18, and TC-19

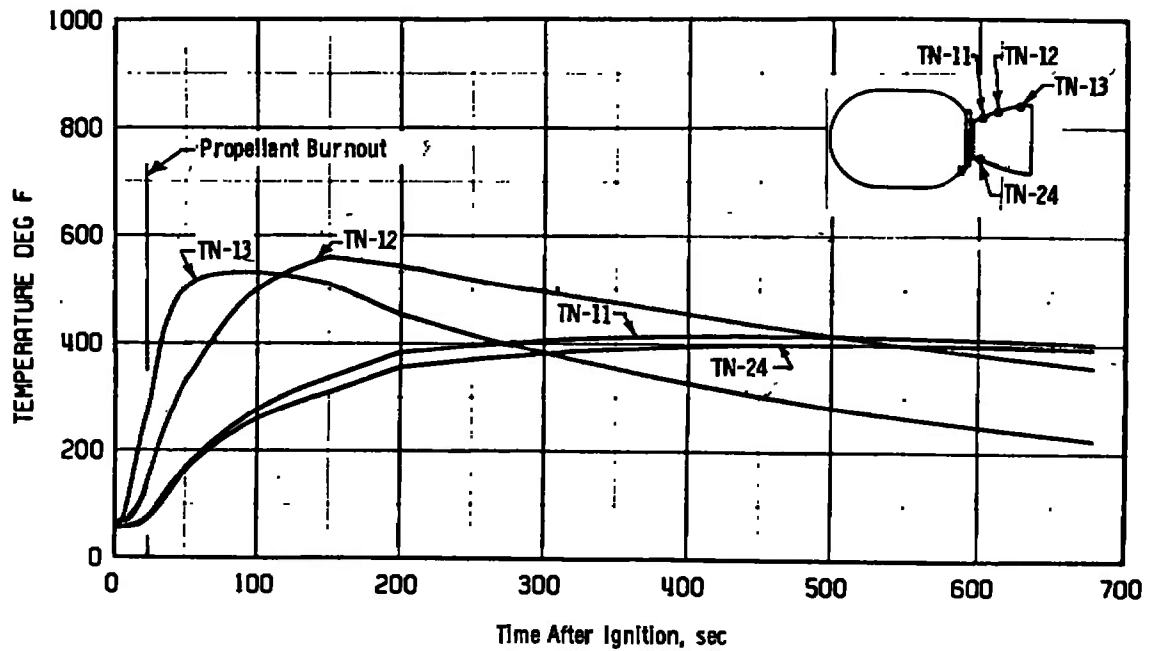


d. Motor Case; TC-7, TC-8, TC-20, and TC-21

Fig. 9 Continued

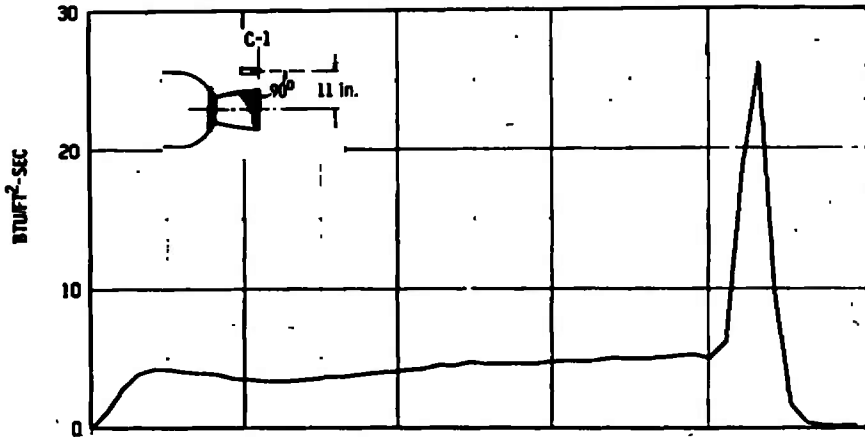


e. Motor Case; TC-9, TC-10, TC-14, TC-22, and TC-23

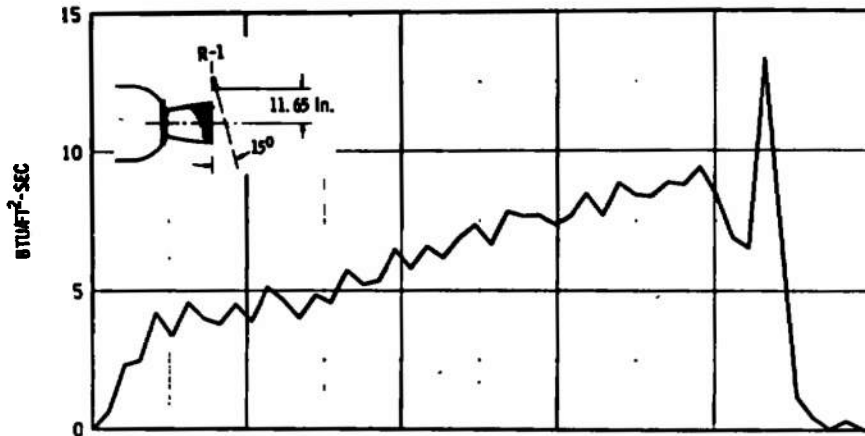


f. Nozzle; TN-11, TN-12, TN-13, and TN-24

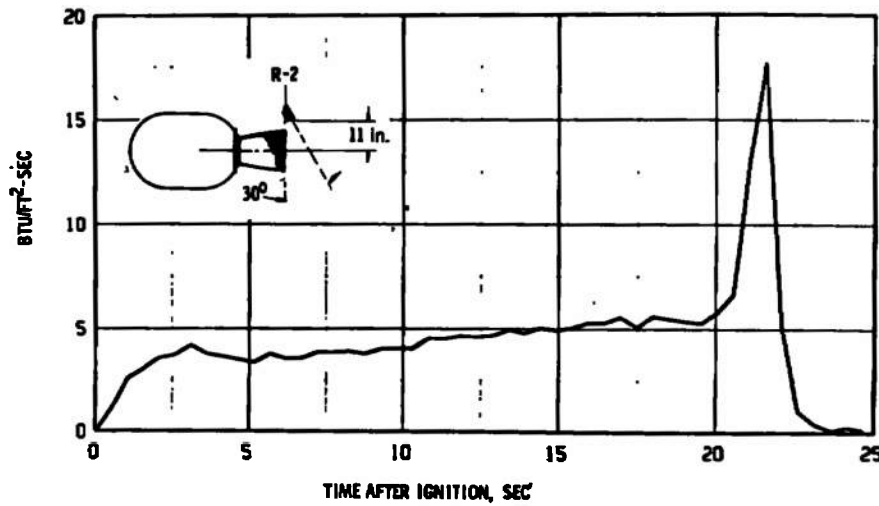
Fig. 9 Concluded



a. Calorimeter, C-1 (View Angle = 140 deg)

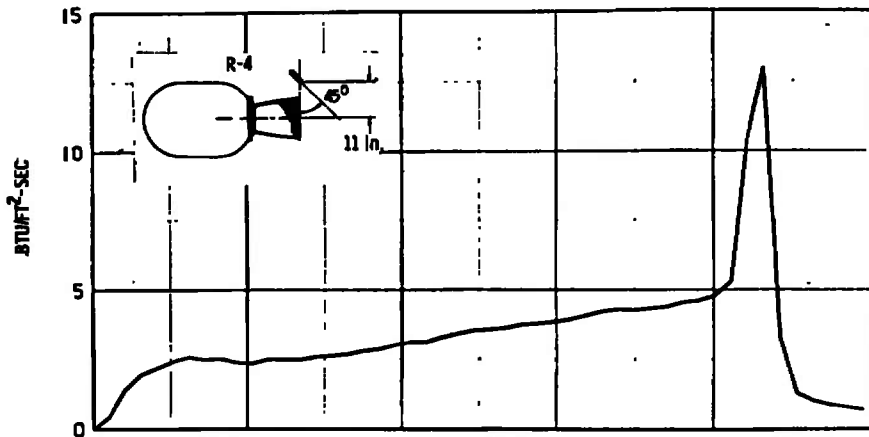


b. Radiometer, R-1 (View Angle = 30 deg)

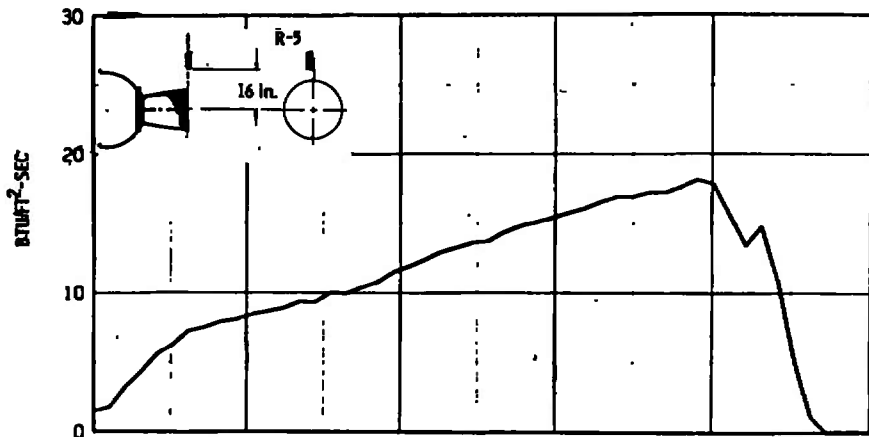


c. Radiometer, R-2 (View Angle = 60 deg)

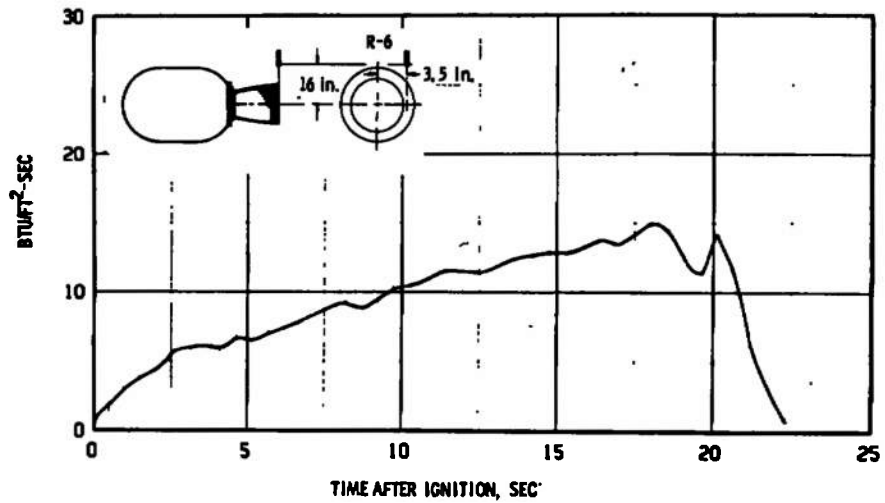
Fig. 10 Exhaust Plume Radiation Variations with Time



d. Radiometer, R-4 (View Angle = 90 deg)

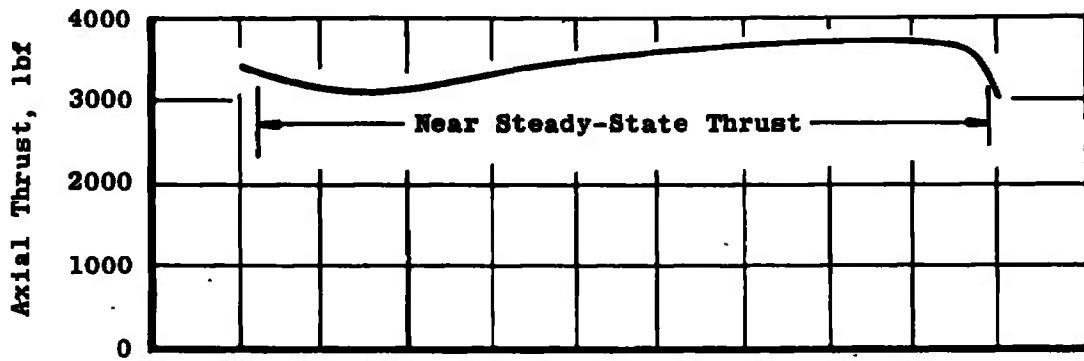


e. Radiometer, R-5 (View Angle = 3 deg)

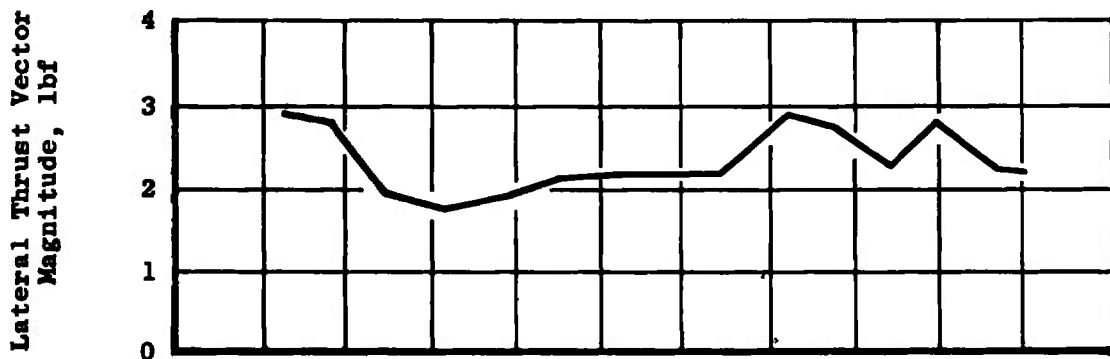


f. Radiometer, R-6 (View Angle = 3 deg)

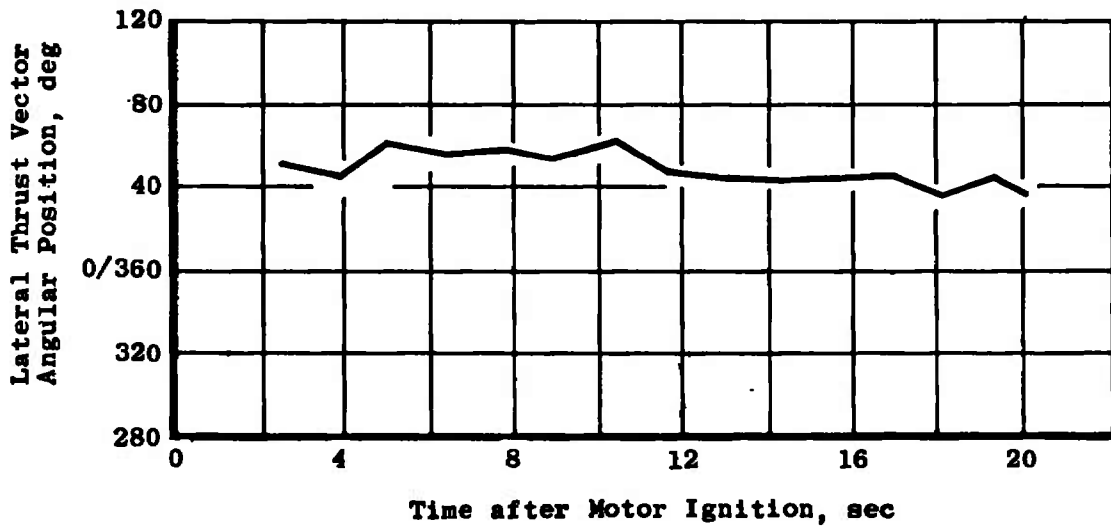
Fig. 10 Concluded



a. Axial Thrust



b. Lateral (Nonaxial) Thrust Vector Magnitude



c. Lateral (Nonaxial) Thrust Vector Angular Position

Fig. 11 Space-Time Variation of Magnitude and Angular Position of Lateral (Nonaxial) Thrust Vector

**TABLE I  
INSTRUMENTATION SUMMARY AND MEASUREMENT UNCERTAINTY**

Parameter Designation	STEADY-STATE ESTIMATED MEASUREMENT*								Range	Type of Measuring Device	Type of Recording Device	Method of System Calibration
	Precision Index (S)			Bias (B)		Uncertainty $\pm(B + t_{0.95}S)$						
	Percent of Reading	Unit of Measurement	Degree of Freedom	Percent of Reading	Unit of Measurement	Percent of Reading	Unit of Measurement					
Axial Force, lbf	±0.126	---	315	+0.1	---	±0.35	---	3000 to 4000 lbf	Bonded Strain-Gage-Type Force Transducers	Voltage-to-Frequency Converter onto Magnetic Tape	In-Place Application of Deadweights Calibrated in the Standards Laboratory	
Total Impulse, lbf-sec	±0.112	---	31	±0.1	---	±0.32	---					
Chamber Pressure, psia	±0.084	---	104	±0.1	---	±0.29	---	500 to 760 psia	Bonded Strain-Gage-Type Pressure Transducers	↓	Resistance Shunt Based on the Standards Laboratory Determination of Transducer Applied Pressure versus Resistance Shunt Equivalent Pressure Relationship	
Chamber Pressure Integral, psia-sec	±0.07	---	31	±0.1	---	±0.24	---					
Low-Range Chamber Pressure, psia	±(0.1% + 0.002 psia)		31	---	±0.008 psia	±(0.2% + 0.012 psia)		4.0 to 4.0 psia				
	±(0.1% + 0.002 psia)		31	±0.2	---	±(0.4% + 0.004 psia)		4.0 to 40 psia				
Test Cell Pressure, psia	±0.23	---	208	±1.25	---	±1.7	---	0.8 to 0.12 psia	Unbonded Strain-Gage-Type Pressure Transducers			
Test Cell Pressure Integral, psia-sec	±0.22	---	31	±1.25	---	±1.7	---					
Motor Temperature, °F	---	±0.25°F	95	---	±2.2°F	---	±2.7°F	0 to 600°F	Chromel-Alumel Temperature Transducers	Sequential Sampling Millivolt-to-Digital Converter, and Magnetic Tape Storage Data Acquisition System	Millivolt Substitution Based on the NBS Temperature versus Millivolt Tables	
Exhaust Plume Heat Flux, Btu/ft <sup>2</sup> -sec	---	---	---	±0.77	---	±0.77 Note 1	---	0 to 6 Btu/ft <sup>2</sup> -sec	Asymptotic Calorimeter		Millivolt Substitution Based on User-Furnished Calibration Curve	
Time Interval, msec	---	±0.25 msec	31	---	±0.01 msec	---	±0.5 msec	---	Time Pulse Generator	Photographically Recording Galvanometer Oscillograph	Time Pulse Generator Calibrated in the Standards Laboratory	
Weight, lbm	---	±0.125 msec	31	---	±0.02 lbm	---	±0.27 lbm	200 to 500 lbm	Beam-Balance Scales	Visual Readout	In-Place Application of Deadweights Calibrated in the Standards Laboratory	
Lateral Thrust Vector Magnitude, lbf	---	±0.12 lbf	11	---	±0.31 lbf	---	±0.57 lbf	1.7 to 2.95 lbf	Bonded-Strain-Gage-Type Force Transducers	Sequential Sampling Millivolt-to-Digital Converter, and Magnetic Tape Storage Data Acquisition System	In-Place Application of Multiple Force Levels Measured with Force Transducers Calibrated in the Standards Laboratory	

\*Reference: CPIA No. 160, "ICRPG Handbook for Estimating the Uncertainty in Measurements made with Liquid Propellant Rocket Engine Systems," April 30, 1969.

Note 1: Uncertainty estimate for this parameter does not include User-furnished calorimeter.

**TABLE II**  
**SUMMARY OF TE-M-521 MOTOR PERFORMANCE**

Test Number	RA182-01	Ref. 2	Ref. 3	Ref. 3	Ref. 4
Motor Serial Number	PV32-248-2	PV32-222-48	PV32-28-2	PV32-28-4	PV-16-907-34
Test Date	07-28-72	01-20-72	7-26-68	6-1-68	4-11-69
Average Motor Spin Rate during Firing, rpm	46	46	100	100	100
Motor Case Temperature at Ignition, °F	40	40	40	100	40
Number of Pyrogen Igniters Utilized	2	2	2	2	2
Ignition Lag Time ( $t_l$ ), sec <sup>(1)</sup>	0.006	0.002	0.006	0.002	0.008
Ignition Time ( $t_i$ ), sec <sup>(2)</sup>	0.110	---	---	---	---
Time from Ignition until Diffuser Flow Breakdown ( $t_{bd}$ ), sec	20.20	21.10	20.30	18.80	20.20
Action Time ( $t_a$ ), sec <sup>(3)</sup>	20.68	21.26	21.242	19.673	21.166
Time Interval that Nozzle Throat Flow was Sonic ( $t_{is}$ ), sec <sup>(4)</sup>	21.63	27.47	38.30	36.90	33.30
Simulated Altitude at Ignition, ft	115,000	121,000	111,000	110,000	113,000
Average Simulated Altitude during $t_a$ , ft	108,000	108,000	113,000	115,000	117,000
Measured Total Impulse (Based on $t_{hd}$ ), lbf-sec					
Average of Four Channels of Data	70,831	70,801	70,015	70,240	70,448
Maximum Channel Deviation from Average, percent	0.040	0.024	0.059	0.006	0.053
Chamber Pressure Integral (Based on $t_{bd}$ ), psia-sec					
Average of Two Channels of Data	13,072	13,214	13,047	13,071	(B)
Maximum Channel Deviation, percent	0.030	0.053	0.17	(A)	---
Cell Pressure Integral (Based on $t_{bd}$ ), psia-sec					
Average of Three Channels of Data	2,3628	2,3038	1,8279	1,5301	1,5224
Maximum Channel Deviation, percent	0.40	3.67	0.18	0.35	0.645
Vacuum Total Impulse (Based on $t_a$ ), lbf-sec	71,231	71,254	71,369	71,513	71,607
Vacuum Total Impulse (Based on $t_{is}$ ), lbf-sec	71,469	71,671	71,600	71,765	71,879
Vacuum Specific Impulse (Based on $t_a$ ), lbf-sec/lbm					
Based on the Manufacturer's Stated Propellant Weight	288.12	288.19	288.94	289.53	289.91
Based on Expended Mass (AEDC)	287.80	285.16	285.37	285.78	287.14
Vacuum Specific Impulse (Based on $t_{is}$ ), lbf-sec/lbm					
Based on the Manufacturer's Stated Propellant Weight	289.08	289.81	289.88	290.55	291.01
Based on Expended Mass (AEDC)	288.76	286.83	286.29	286.79	288.23
Average Vacuum Thrust Coefficient, $C_F$					
Based on $t_a$ and Average Pre- and Postfire Areas	1.856	1.838	1.840	1.841	(B)

(1) Defined as the time interval from application of ignition voltage to the first perceptible rise in chamber pressure.

(2) Defined as the time interval from application of ignition voltage to attainment of 90 percent of peak thrust during the ignition transient.

(3) Defined as the time interval beginning when chamber pressure has risen to 10 percent of maximum at ignition and ending when chamber pressure has fallen to 10 percent of maximum during tailoff.

(4) Defined as the time interval between the first indication of chamber pressure at ignition and the time at which the ratio of chamber to cell pressure has decreased to 1.3 during tailoff.

(A) One channel of chamber pressure utilized.

(B) Chamber pressure data invalid from 3.5 to 18.0 sec after ignition.

**TABLE III**  
**SUMMARY OF TE-M-521 MOTOR PHYSICAL DIMENSIONS**

Test Number	RA182-01	Ref. 2	Ref. 3	Ref. 3	Ref. 4
Motor Serial Number	PV32-248-2	PV32-222-48	PV32-28-2	PV32-28-4	PV-16-907-34
Test Date	7/28/72	1/20/72	7/26/68	8/1/68	4/11/69
Motor Spin Rate, rpm	46	46	100	100	100
AEDC Prefire Motor Weight, lbm	442.340*	473.250	274.612	274.649	275.713
AEDC Postfire Motor Weight, lbm	194.840*	223.375	24.516	24.410	26.335
AEDC Expended Mass, lbm	247.500	249.875	250.096	250.239	249.378
Manufacturer's Stated Propellant Weight, lbm	247.2	247.30	247.0	247.0	247.0
Nozzle Throat Area, in.					
Prefire	2.790**	2.790	2.7907	2.7847	2.7877
Postfire	3.082	3.076	3.0697	3.0757	3.1201
Change from Prefire Measurement, percent	+10.5	+10.3	+9.997	+10.450	+11.803
Nozzle Exit Area, in.					
Prefire	148.53	148.41	148.574	148.682	148.396
Postfire	147.02	147.23	146.858	146.483	147.763
Change from Prefire Measurement, percent	-1.02	-0.8	-1.155	-0.806	-0.4265

\*Includes igniter weight and thrust adapter

\*\*Supplied by motor manufacturer

UNCLASSIFIED

Security Classification

DOCUMENT CONTROL DATA - R & D

(Security classification of title, body of abstract and indexing annotation must be entered when the overall report is classified)

1 ORIGINATING ACTIVITY (Corporate author) Arnold Engineering Development Center Arnold Air Force Station, Tennessee 37389		2a. REPORT SECURITY CLASSIFICATION UNCLASSIFIED	
		2b. GROUP N/A	
3 REPORT TITLE DESIGN ASSURANCE TEST OF THE THIOKOL TE-M-521-5 APOGEE KICK MOTOR TESTED IN THE SPIN MODE AT SIMULATED ALTITUDE CONDITIONS			
4 DESCRIPTIVE NOTES (Type of report and inclusive dates) July 28, 1972--Final Report			
5 AUTHOR(S) (First name, middle initial, last name) A. A. Cimino, ARO, Inc.			
6 REPORT DATE March 1973	7a TOTAL NO OF PAGES 40	7b. NO. OF REFS 7	
8a CONTRACT OR GRANT NO	9a ORIGINATOR'S REPORT NUMBER(S) AEDC-TR-73-15		
b. PROJECT NO	9b OTHER REPORT NO(S) (Any other numbers that may be assigned this report) ARO-ETF-TR-72-177		
c. Program Element 921E3			
d			
10 DISTRIBUTION STATEMENT Approved for public release; distribution unlimited.			
11 SUPPLEMENTARY NOTES Available in DDC		12 SPONSORING MILITARY ACTIVITY NASA-GSFC Greenbelt Maryland 20771	
13 ABSTRACT One Thiokol Chemical Corporation TE-M-521-5 solid-propellant apogee rocket motor was successfully fired at an average simulated altitude of about 108,000 ft while spinning at 46 rpm. The general program objectives were to verify compliance of motor performance with the manufacturer's specifications. Specific primary objectives were to determine vacuum ballistic performance of the motor after prefire vibration conditioning and temperature conditioning at 40°F, altitude ignition characteristics, motor structural integrity, and motor temperature-time history during and after motor operation. Additional objectives were to measure the lateral (nonaxial) thrust component during motor operation and to measure radiation heat flux in the vicinity of the nozzle exit plane.			

**UNCLASSIFIED**

Security Classification

14. KEY WORDS	LINK A		LINK B		LINK C	
	ROLE	WT	ROLE	WT	ROLE	WT
rocket motor solid propellants space vehicle altitude simulation performance structural stability ignition ballistics spin stabilization						

AFIC  
April 1975 Form

**UNCLASSIFIED**

Security Classification